Lensing and AMiBA Studies of Galaxy Clusters

Keiichi Umetsu, ASIAA, Taiwan

@TIARA Winter School: 28.01.2010

Contents

1. **Introduction – Galaxy Clusters**
2. **Gravitational Lensing Theory**
3. **Cluster Weak Gravitational Lensing**
   - Quadrupole Image Distortions
   - Cluster Weak Lensing Profiles
   - Lens Magnfication Bias
4. **The Y-T Lee AMiBA Project**
   - **CMB Interferometers**
   - **Highlights of AMiBA-7 Sciences**
5. **Summary**

1. Introduction: Galaxy Clusters?

Concordance Structure Formation Scenario

Standard Lambda Cold DM (=ΛCDM) Paradigm:

- **Initial conditions**, precisely known from linear theory & CMB+ data (@ z = z_dec ~ 1100)
- 80% of our *material universe* is composed of dark matter
- Use an **N-body simulation** (+linear theory) to study hierarchical structure formation (0 < z < 1100)
- **Bottom-up nature**: smaller objects first formed, then larger ones form via mergers and mass-accretions

WMAP5yr+

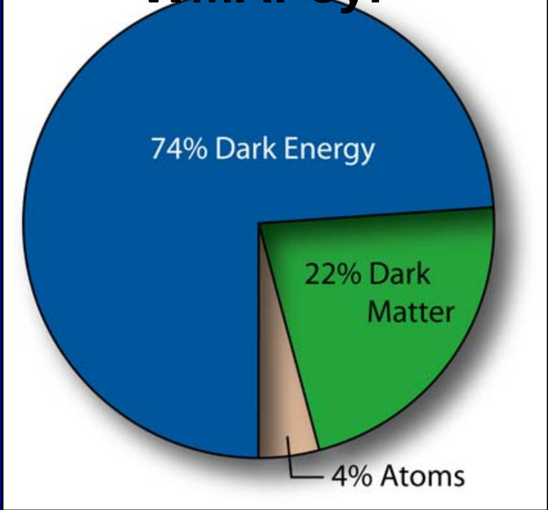

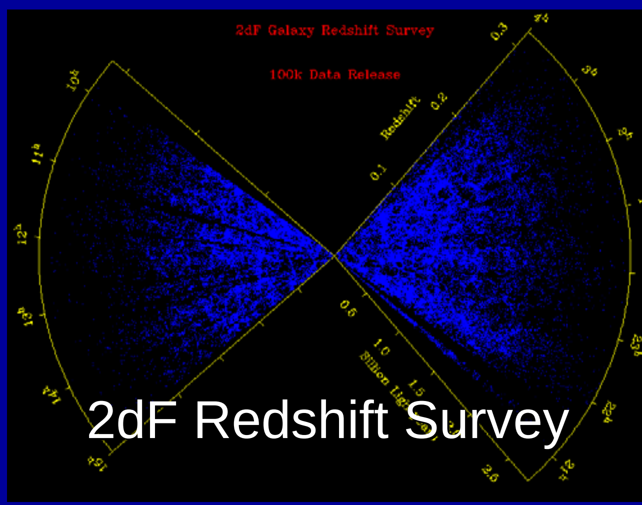

2dF Redshift Survey

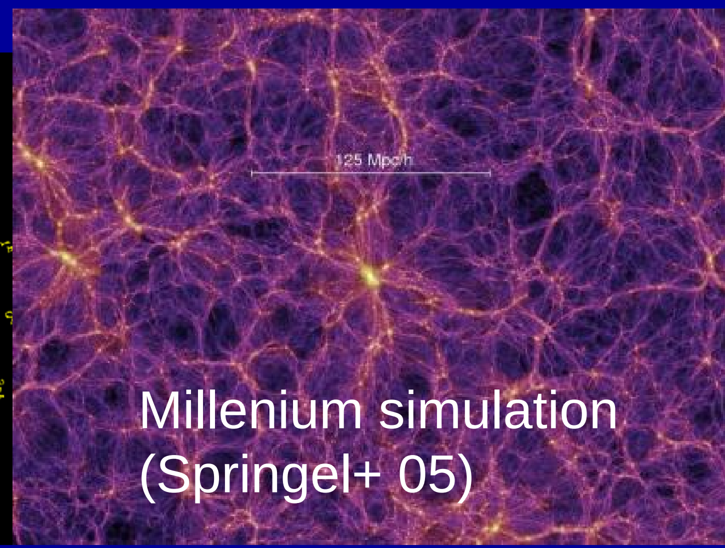

Millenium simulation (Springel+ 05)

Observed Matter P(k) vs. ΛCDM

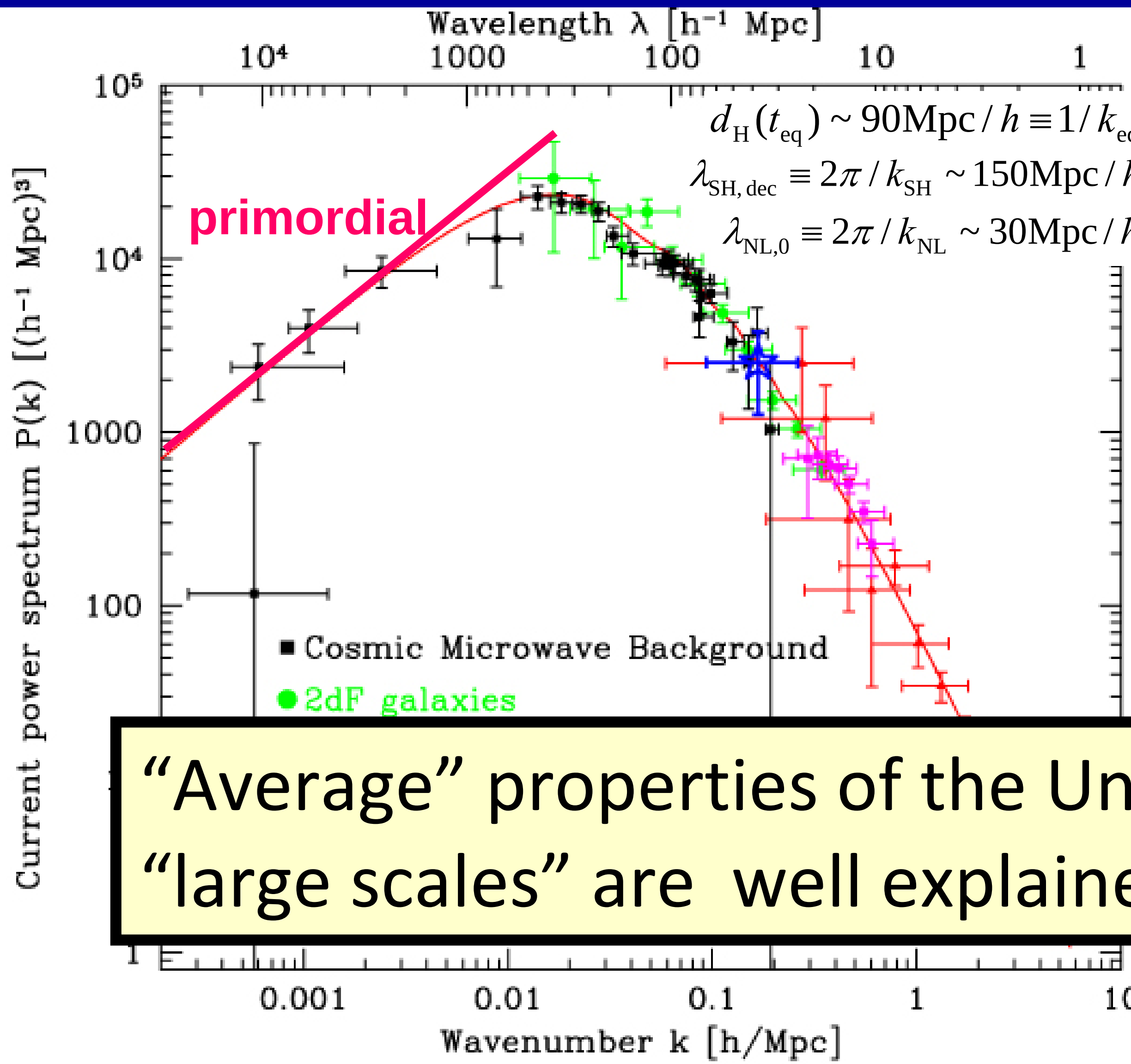

$d_{\rm H}(t_{\rm eq}) \sim 90{\rm Mpc}/h \equiv 1/k_{\rm eq}$

$\lambda_{\rm SH,\,dec} \equiv 2\pi/k_{\rm SH} \sim 150{\rm Mpc}/h$

$\lambda_{\rm NL,0} \equiv 2\pi/k_{\rm NL} \sim 30{\rm Mpc}/h$

Tegmark & Zaldarriaga 2002

P(k) = Ak^n with n ~ 1
@ k<< keq~0.01h/Mpc

Turn-over @ k~keq

P(k)=Ak^(n-4) at k>>keq
due to the decay of Φ(k)
on sub-horizon scales in
the radiation era

Baryon acoustic oscillation

les,

“Average” properties of the Universe on “large scales” are well explained by ΛCDM

Large Scale Structure in the Universe

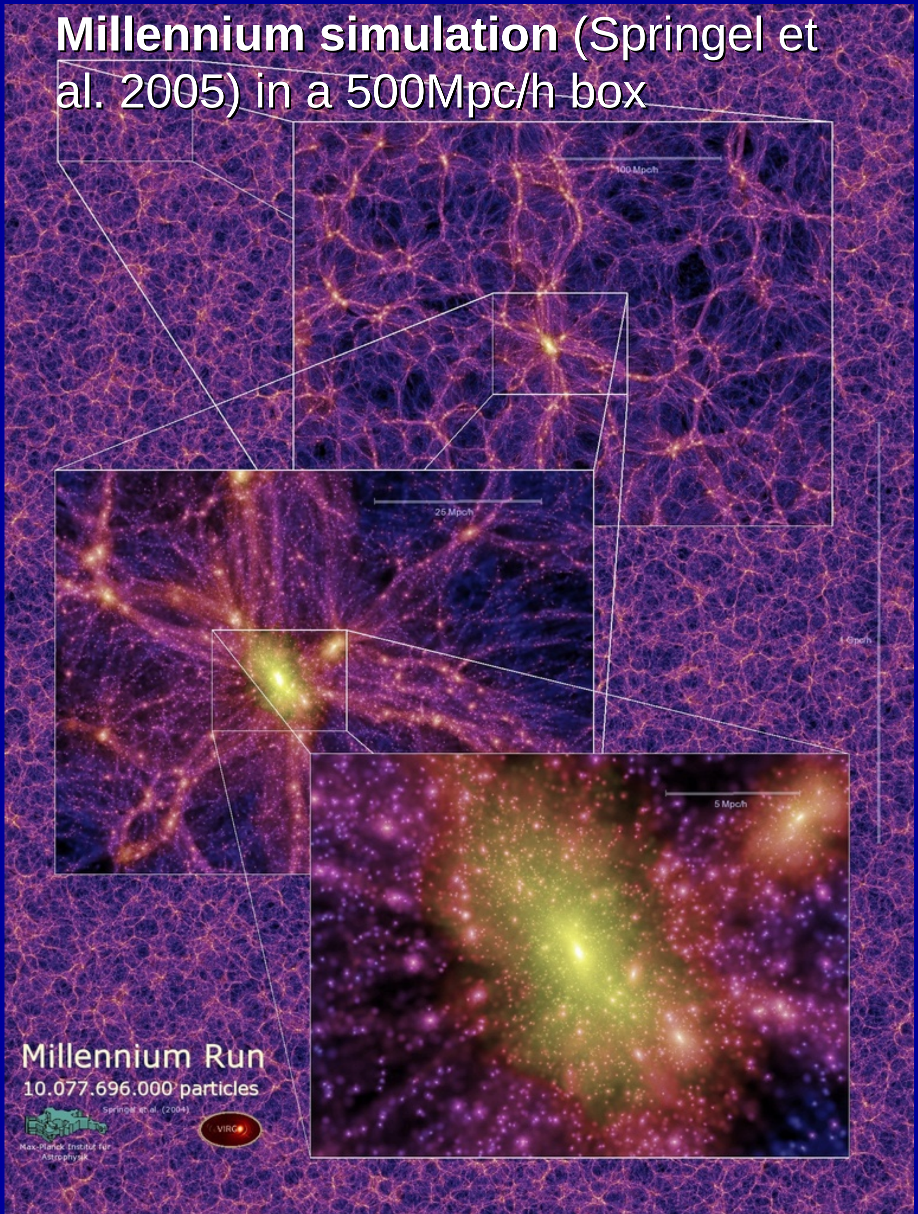

Millennium simulation (Springel et al. 2005) in a 500Mpc/h box

N-body simulations

Studying "non-linear" structure formation in an expanding Universe after the cosmic decoupling epoch (z~1100) governed by the *gravity*

- Large Scale Structure (LSS): cosmic structure on scales of ~10-50 Mpc/h, representing forming super-clusters, low-density voids, filaments of galaxies
- Clusters of galaxies: non-linear, most massive gravitationally bound structure of R=(1-2) Mpc/h, which serve as building blocks of LSS

Galaxy Clusters – Building Blocks of LSS

Galaxy Clusters – identified as dense nodes of "Cosmic Web"

Typical mass: $M_{vir} \sim 10^{14-15}\ M_{sun}\ /h$

Distribution of discrete galaxies

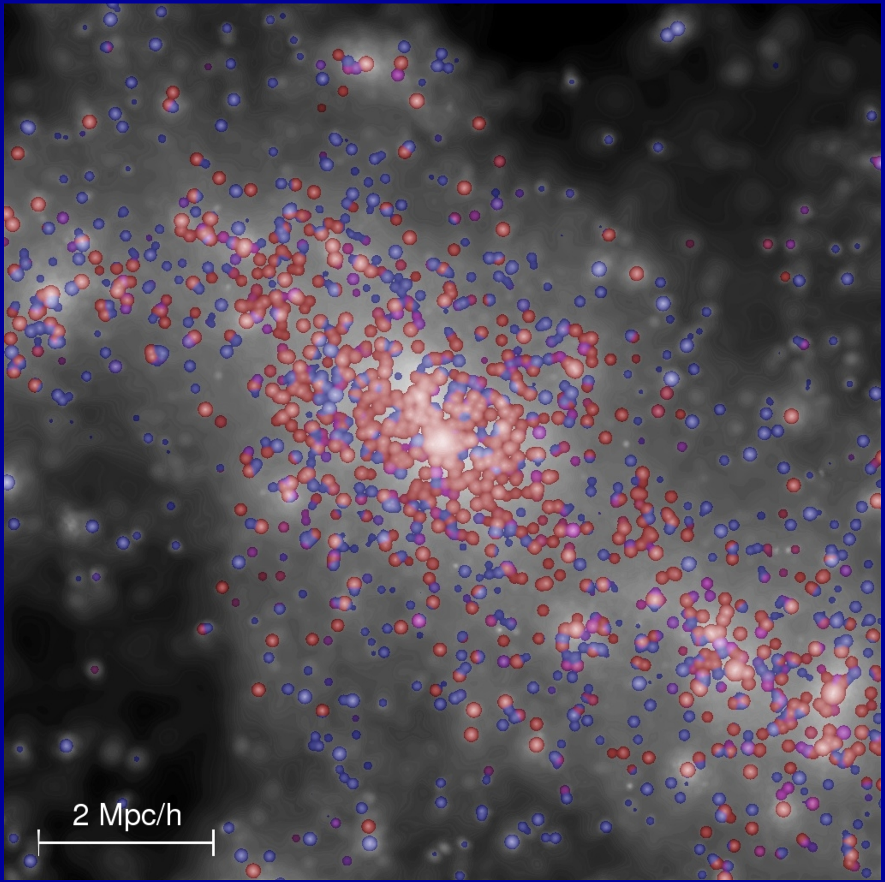

Distribution of underlying DM (~mass)

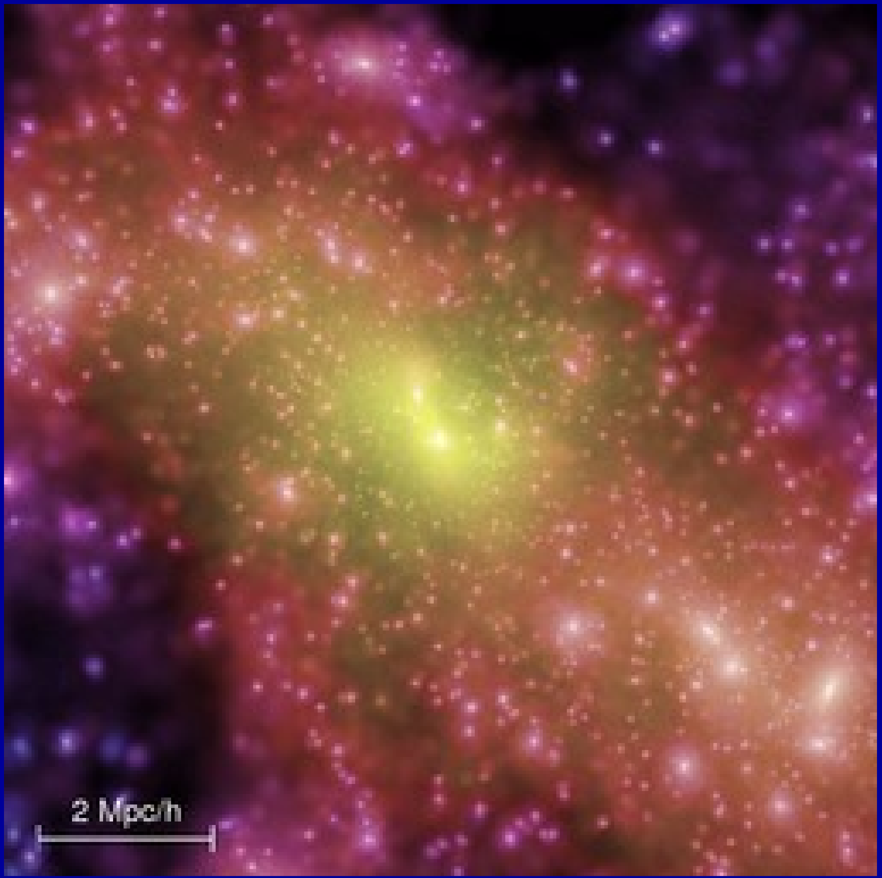

From Millennium Simulation

Clusters as

A1689 (z=0.18

- *Subaru*
  Suprime-C
  34’x27’

- *HST ACS*
  3.3’x3.3’
- *Chandra* ACIS
- AMiBA
- VLT/VIRMOS
- Suzaku/XIS

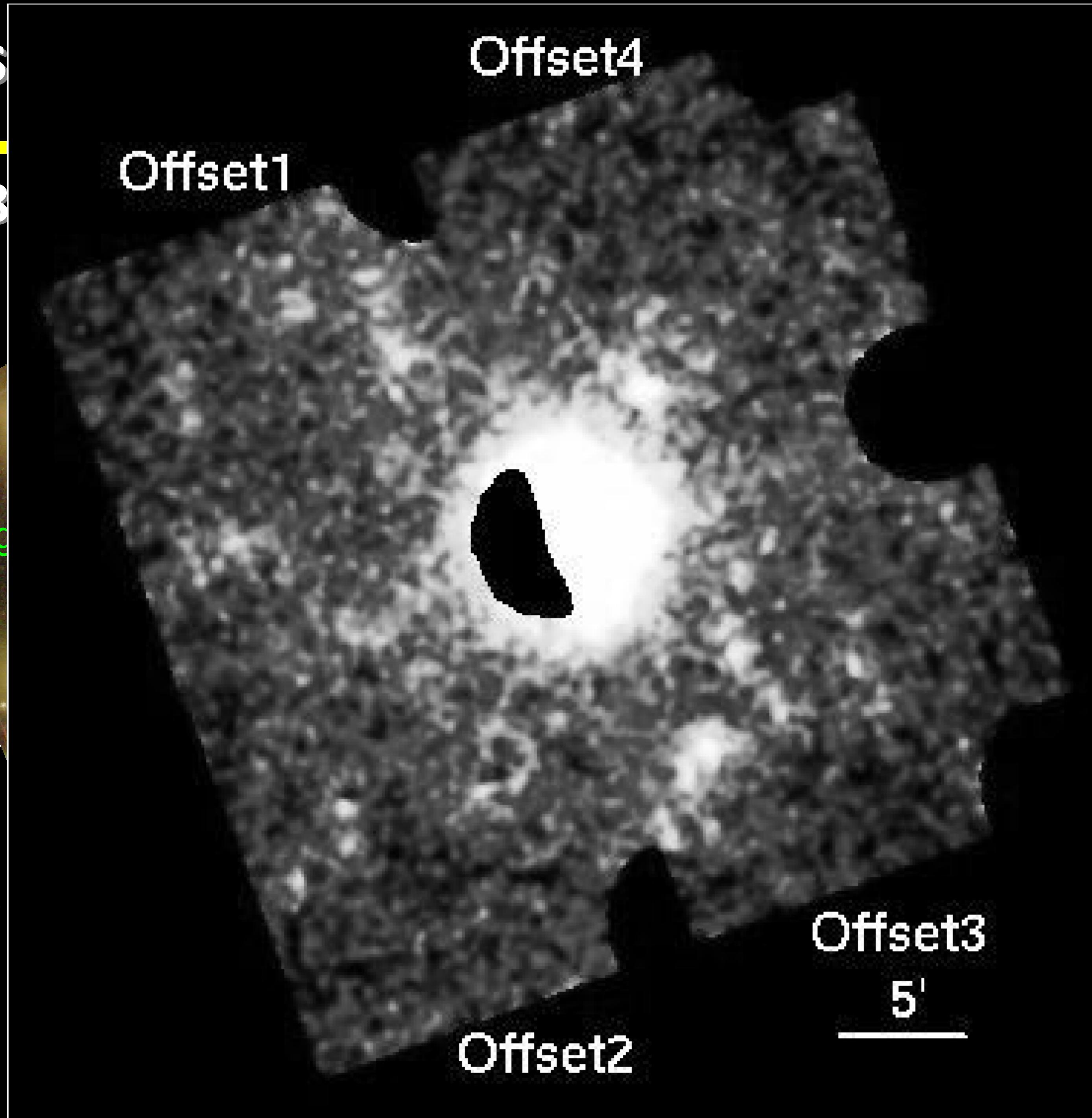

2. Gravitational Lensing Theory

My lecture notes on

"Cluster Weak Gravitational Lensing"

from "Enrico-Fermi Summer School 2008, Italy" found @

http://www.asiaa.sinica.edu.tw/~keiichi/upfiles/umetsu_fermi08.pdf

Theoretical backgrounds and basic concepts on cosmological lensing and observational techniques are summarized in these lecture notes.

Importance of Gravitational Lensing

Gravitationally-lensed images of background galaxies carry the imprint of $\Phi(x)$ of intervening cosmic structures:

Observable weak shape distortions can be used to derive the distribution of matter (i.e., mass) in a model independent way!!

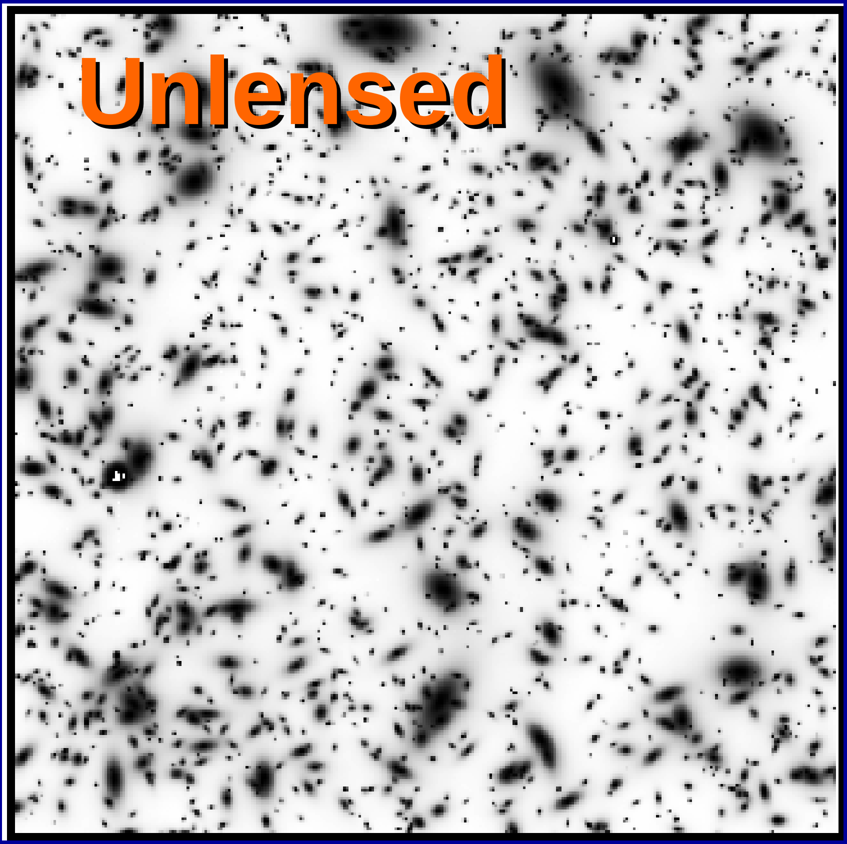

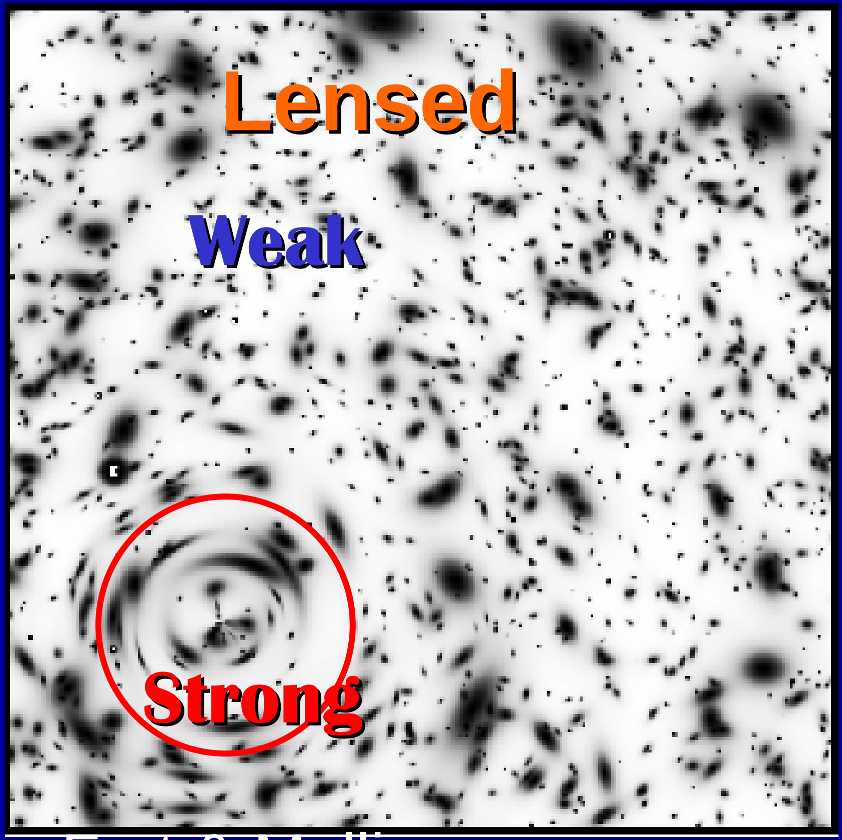

Fort & Mellier

Gravitational Bending of Light Rays

Gravitational deflection angle in the weak-field limit (|Φ|/c^2<<1)

Light rays propagating in an inhomogeneous universe will undergo **small transverse excursions** along the photon path: i.e., **light deflections**

Bending angle

$$\delta\hat{\alpha} \approx \frac{\delta p_{\perp}}{p_{\parallel}} = -\frac{2}{c^2}\nabla_{\perp}\Psi(x_{\parallel}, x_{\perp})\delta x_{\parallel}$$

Small transverse excursion of photon momentum

$$\hat{\alpha}^{\mathrm{GR}} = 2\hat{\alpha}^{\mathrm{Newton}} \rightarrow \frac{4GM}{c^2 r} = 1.''75\left(\frac{M}{M_{sun}}\right)\left(\frac{r}{R_{sun}}\right)^{-1}$$

Lens Equation (for cluster lensing)

Lens equation (Cosmological lens eq. + single/thin-lens approx.)

β: true source position

θ: apparent image position

$$\boldsymbol{\beta} - \boldsymbol{\theta} = \frac{D_{ds}}{D_s}\hat{\boldsymbol{\alpha}}(\boldsymbol{\theta}) \equiv -\nabla\psi(\boldsymbol{\theta})$$

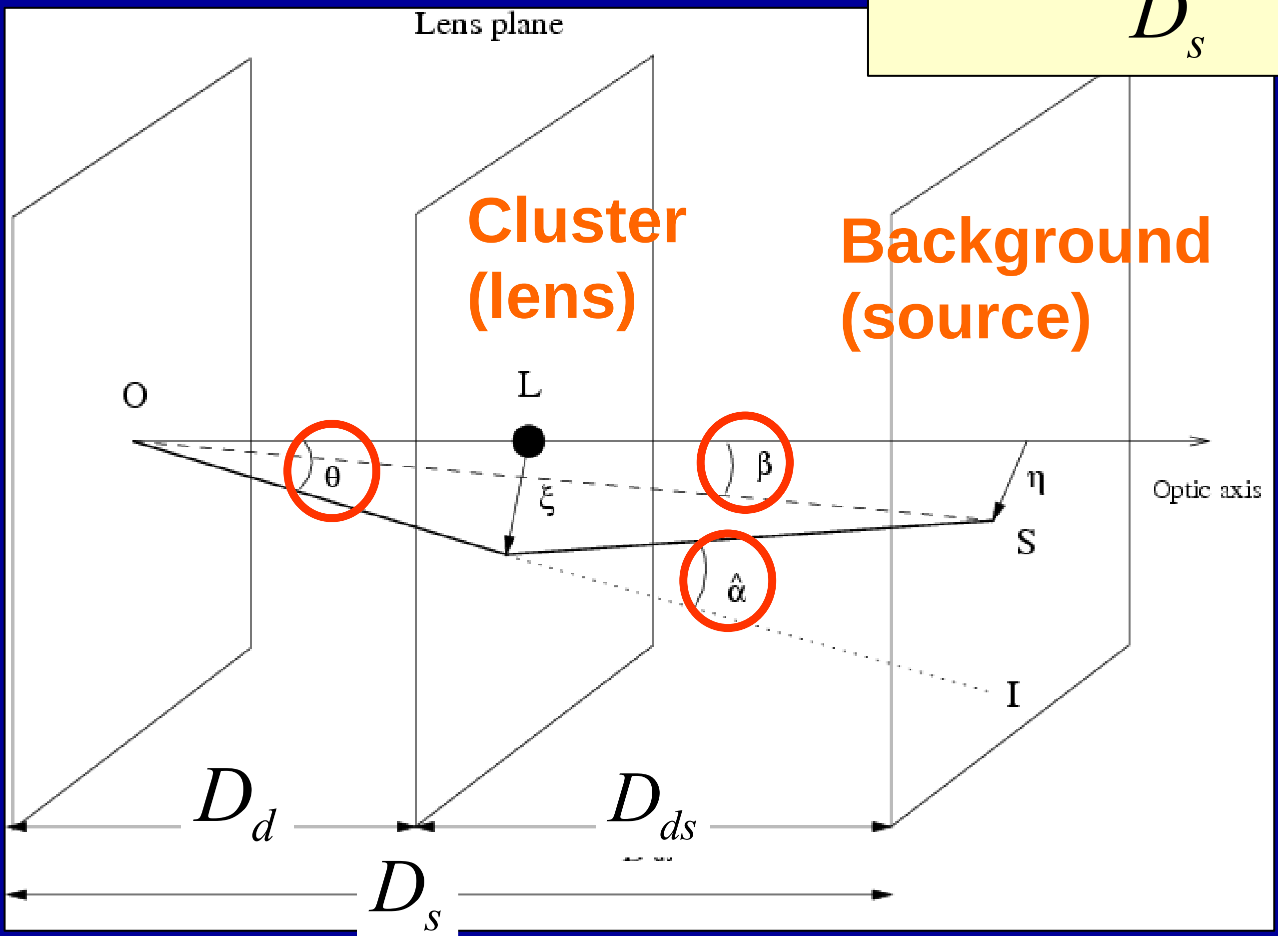

For a rigid derivation of cosmological lens eq., see, e.g., Futamase 95

3. Cluster Weak Lensing

3.1 Quadrupole Weak Lensing

Differential deflection causes a distortion in "**area**" and "**shape**" of an image

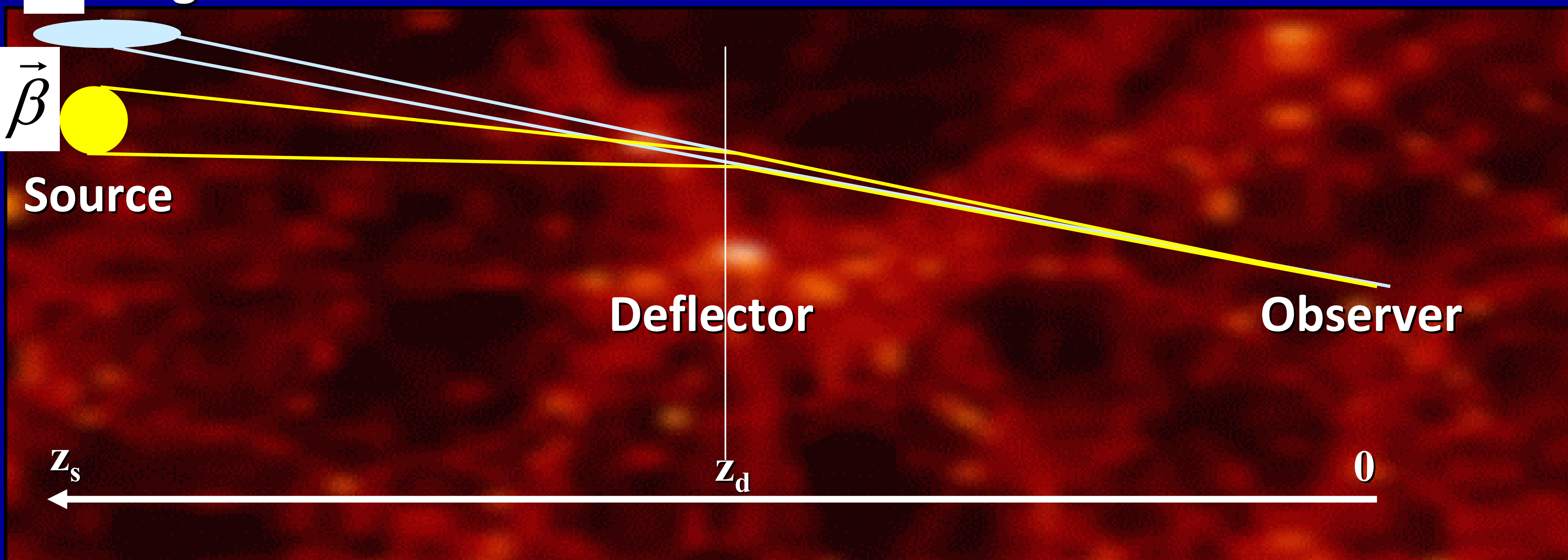

Deformation of shape/area of an image

$$\delta\beta_i = \mathbf{A}_{ij}\delta\theta_j + O(\delta\theta^2)$$

For an infinitesimal source:

$$d^2\vec{\beta} = \mathbf{A}\, d^2\vec{\theta}$$

A: Jacobian matrix of the lens equation

Effects of Convergence and Shear

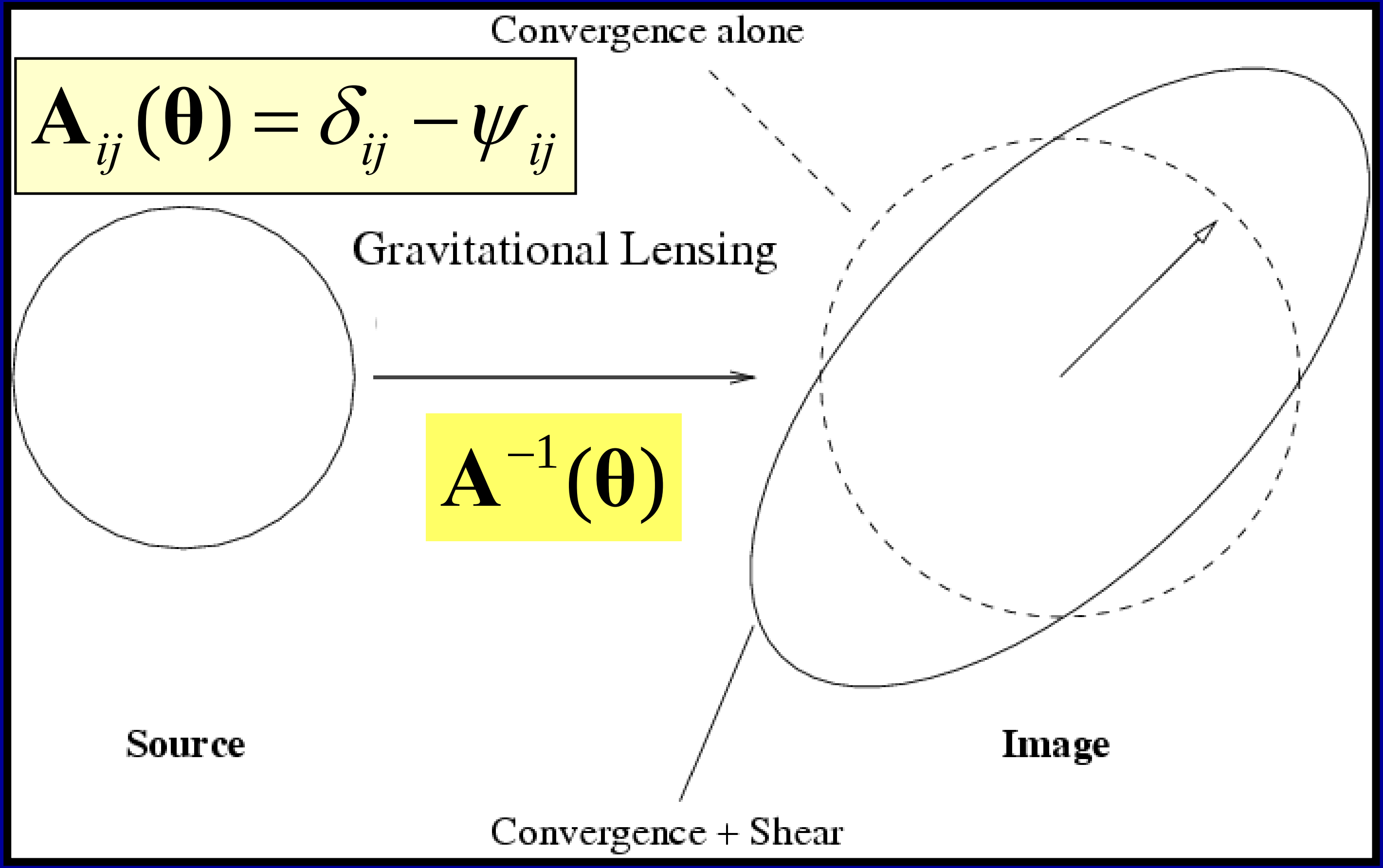

$$\mathcal{A}(\boldsymbol{\theta}) = \begin{pmatrix} 1-\kappa-\gamma_1 & -\gamma_2 \\ -\gamma_2 & 1-\kappa+\gamma_1 \end{pmatrix} = (1-\kappa)\begin{pmatrix} 1 & 0 \\ 0 & 1 \end{pmatrix} - \begin{pmatrix} \gamma_1 & \gamma_2 \\ \gamma_2 & -\gamma_1 \end{pmatrix},$$

Physical Meaning of κ

Lensing Convergence: weighted-projection of mass overdensity

$$\kappa(\boldsymbol{\theta}) \equiv \frac{1}{2}\Delta^{(2)}\psi(\boldsymbol{\theta}) = \int dl\, \delta\rho_m \left(\frac{c^2}{4\pi G} \frac{D_s}{D_d D_{ds}} \right)^{-1} \approx \frac{\Sigma_m(\boldsymbol{\theta})}{\Sigma_{\rm crit}}$$

Critical surface mass density of gravitational lensing

$$\Sigma_{\rm crit}(z_d, z_s; \underline{\Omega_m, \Omega_\Lambda, H_0}) = \frac{c^2}{4\pi G} \frac{D_s}{D_d D_{ds}}$$

probability

- **Strong lensing** κ~1 @ high density regions (r=10kpc-100kpc)
- **Weak lensing** κ~0.1 @ r = 100kpc – a few Mpc in clusters
- **Cosmic shear** κ~1% @ Large Scale Structure (~10Mpc)

Note, this is only a crude definition, as lensing also depends on the (trace-free) tidal shear field.

Geometric Scaling of Lensing Signal

Distnace raito as a function of source z

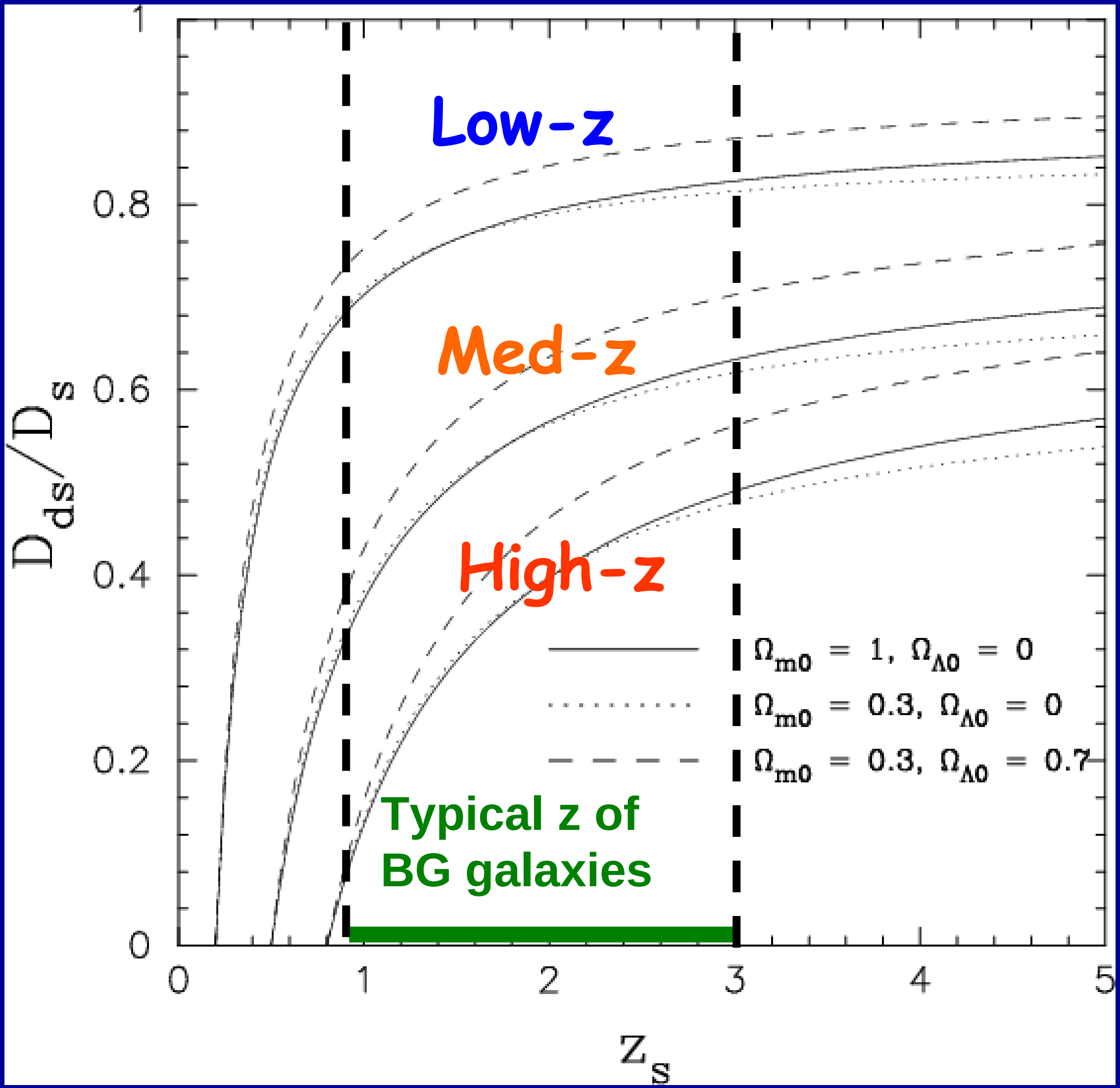

Physical mass to signal units

$$\kappa(\boldsymbol{\theta}) \propto \left(\frac{D_{ds}}{D_s}\right)\Sigma_m(\boldsymbol{\theta})$$

Low-z cluster:

zd=0.2

Med-z cluster:

zd=0.5

High-z cluster:

zd=0.8

Gravitational Shear Field

2x2 shear matrix: Quadrupole shape distortions (2 DoF)

- Coordinate dependent (cf. Stokes Q,U)
- Spin-2 "directional" quantity
- **Observable as an image ellipticity in the WL limit (|κ|,|γ|<<1)**

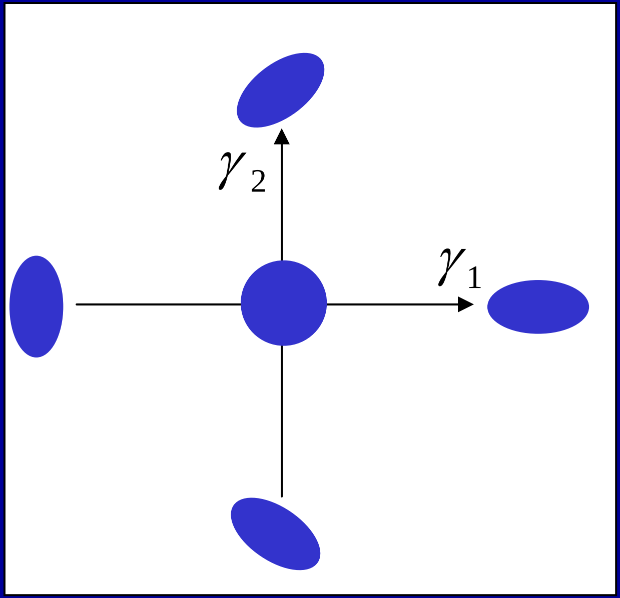

$$\Gamma_{ij} = \begin{bmatrix} +\gamma_1 & \gamma_2 \\ \gamma_2 & -\gamma_1 \end{bmatrix} \Leftrightarrow \begin{bmatrix} +Q & U \\ U & -Q \end{bmatrix}$$

Spin-2 complex shear field

$$\gamma(\boldsymbol{\theta}) = \gamma_1 + i\gamma_2 \equiv |\gamma| e^{2i\phi_\gamma}$$

Measurement of the Shear: Moment Method

Image quadrupoles:

$$Q_{ij} = \langle x_i x_j \rangle$$

Quadrupole moments of the object surface brightness

Complex ellipticity, $e = e_1 + ie_2$:

$$e_1 = \frac{Q_{11} - Q_{22}}{Q_{11} + Q_{22}}, \; e_2 = \frac{2Q_{12}}{Q_{11} + Q_{22}}$$

In the weak limit ($\kappa, |\gamma| << 1$):

Mapping from intrinsic → observed ellipticity

$$e^{\mathrm{obs}} = e^{(s)} + 2\gamma + O(|\gamma|^2)$$

e(s): source intrinsic ellipticity

Assuming that background sources have random orientations:

$$\langle e^{obs} \rangle = 2\gamma + O\left(\frac{\sigma_e}{\sqrt{N}}\right) + O(|\gamma|^2)$$

E and B Mode Distortion Patterns

Shear matrix with 2-DoF can be expressed with 2 scalar potentials (e.g., Crittenden et al. 2002):

Shear matrix in terms of potential:

$$\Gamma_{ij} = \left(\partial_i \partial_j - \frac{1}{2} \delta_{ij} \Delta \right) \psi_E + \frac{1}{2} \left(\varepsilon_{kj} \partial_i \partial_k + \varepsilon_{ki} \partial_j \partial_k \right) \psi_B$$

$$\psi_E = \psi \text{ (lens potential)}$$

$$\psi_B = 0$$

In a pure weak lensing signal,

B-mode = 0 (E>>B)

→ B-mode "signal" can be used to monitor residual systematic effects in lensing measurements:

e.g., residual PSF anisotropies

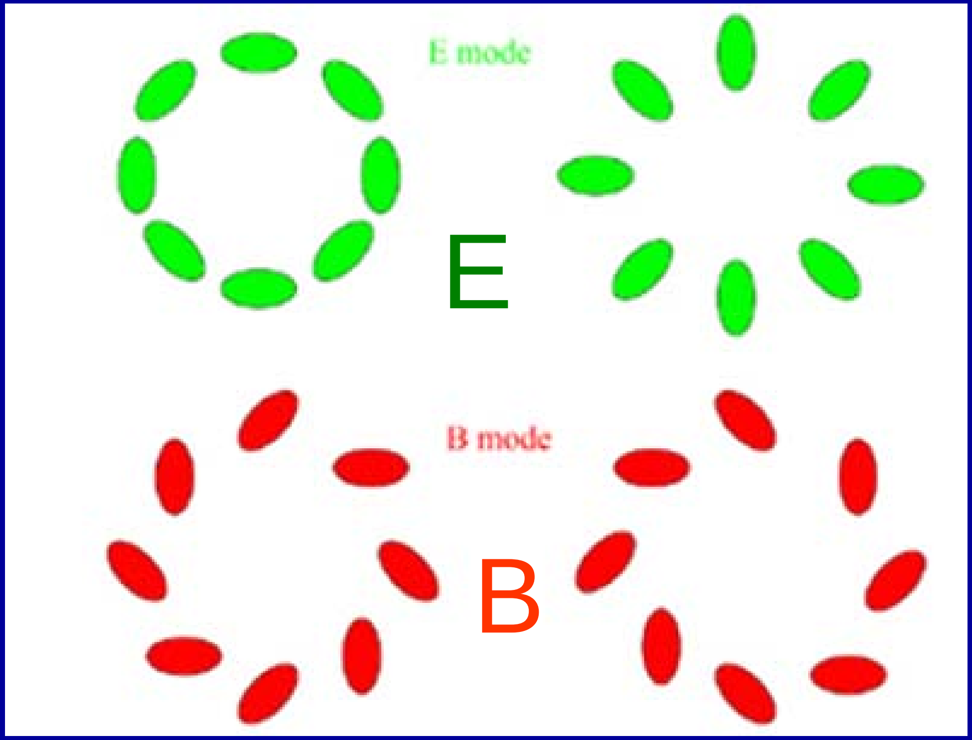

Shear-to-Mass Inversion: Mass Reconstruction

Observable shear field into a 2D mass map: "non-local"

Extract E-mode from shear matrix;

$$\Delta\kappa(\boldsymbol{\theta}) = \partial^i \partial^j \Gamma_{ij}(\boldsymbol{\theta})$$

Then, invert:

$$\kappa(\boldsymbol{\theta}) = \Delta^{-1}(\boldsymbol{\theta}, \boldsymbol{\theta}') * \left(\partial^i \partial^j \Gamma_{ij}(\boldsymbol{\theta}')\right)$$

Kaiser & Squires (1993) Inversion Method:

$$\hat{\kappa}(\vec{l}) = \cos(2\phi_l)\hat{\gamma}_1(\vec{l}) + \sin(2\phi_l)\hat{\gamma}_2(\vec{l}), \quad \vec{l} \neq 0$$

Use the Green function for 2D-Poisson equation:

But l=0 mode (DC-component) is "unconstrained".

Mass-sheet degeneracy
(in the weak lensing limit)

$$\kappa(\boldsymbol{\theta}) \rightarrow \kappa(\boldsymbol{\theta}) + const.$$

Weak Shear Field vs. 2D Mass Map

Cluster z = 0.77; Arc z = 4.89: Photo from H. Yee (HST/ACS)

Observable tangential alignment of background galaxy images, probing the underlying gravitational field of cosmic structure

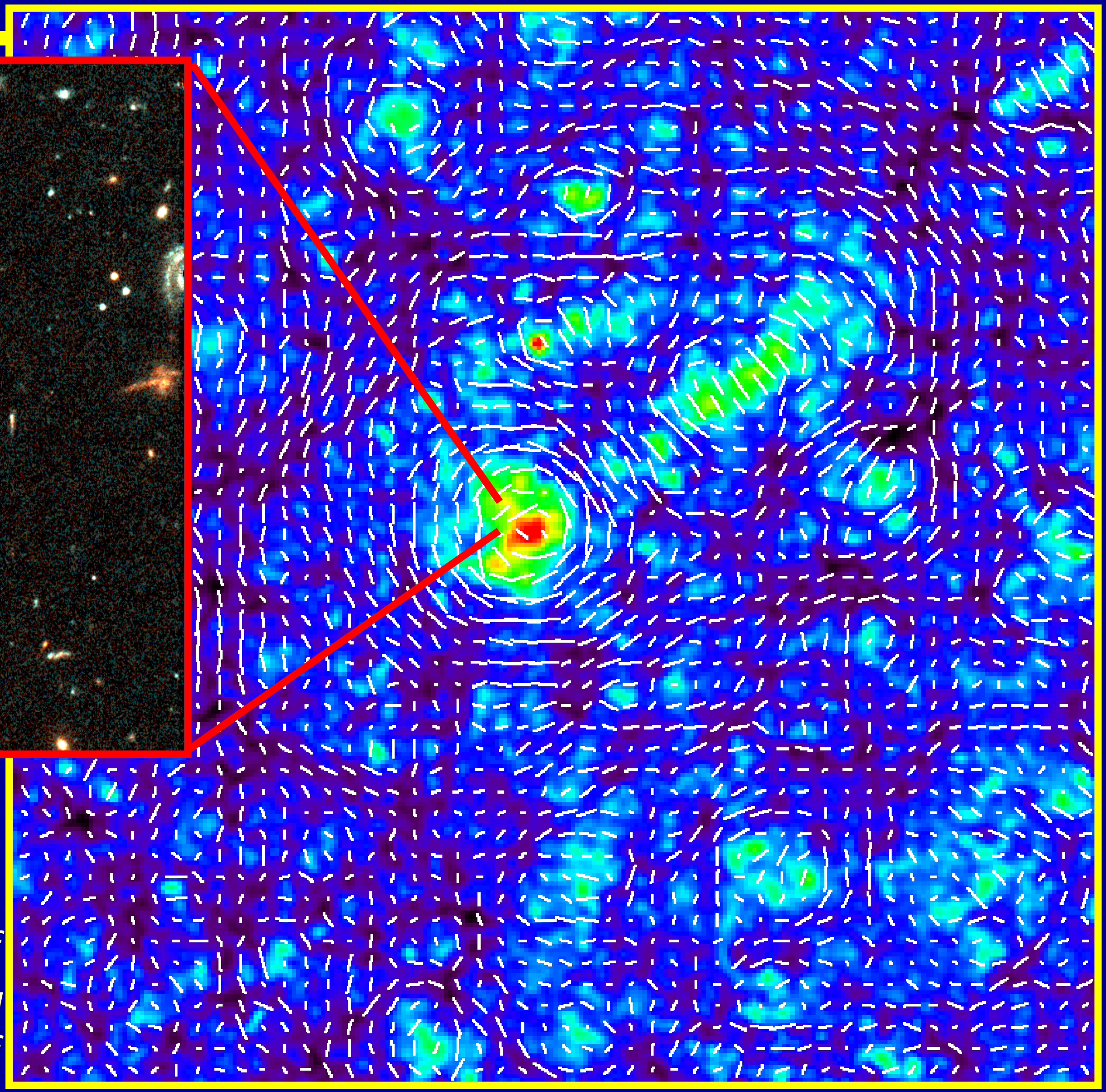

Simulated 3x3 degree field (Hamana 02)

3.2 Cluster Weak Lensing Profiles

Cluster Tangential Distortion

$$\gamma_+(r) \propto \Delta\Sigma_m(r) \equiv \overline{\Sigma}_m(<r) - \Sigma_m(r)$$

Measure of tangential coherence of distortions around the cluster (Tyson & Fisher 1990)

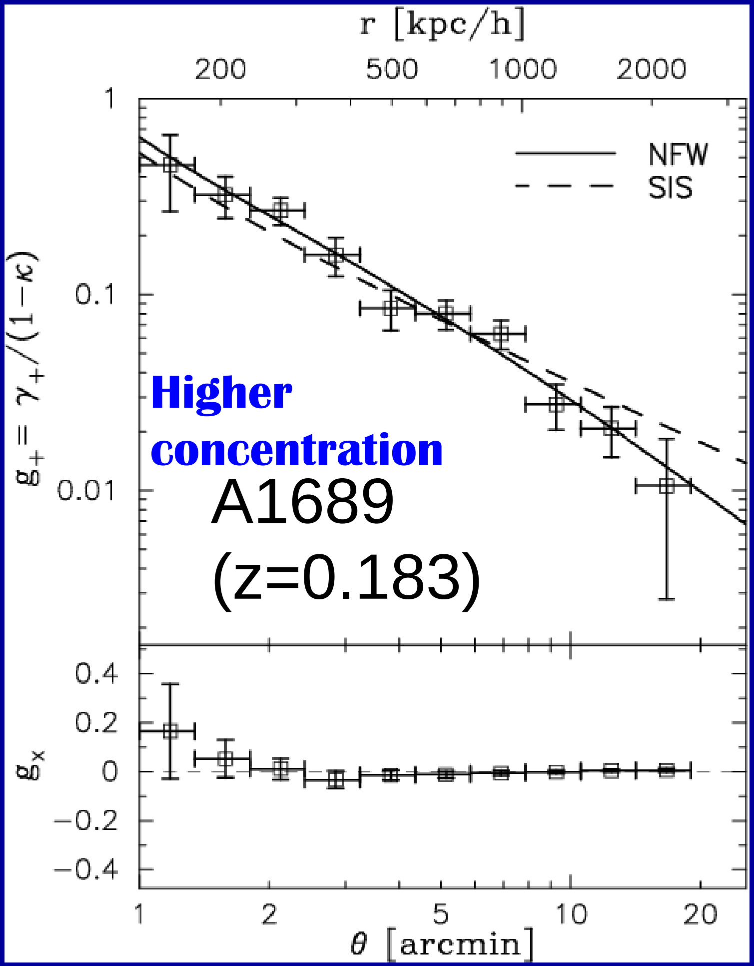

Umetsu & Broadhurst 08, ApJ

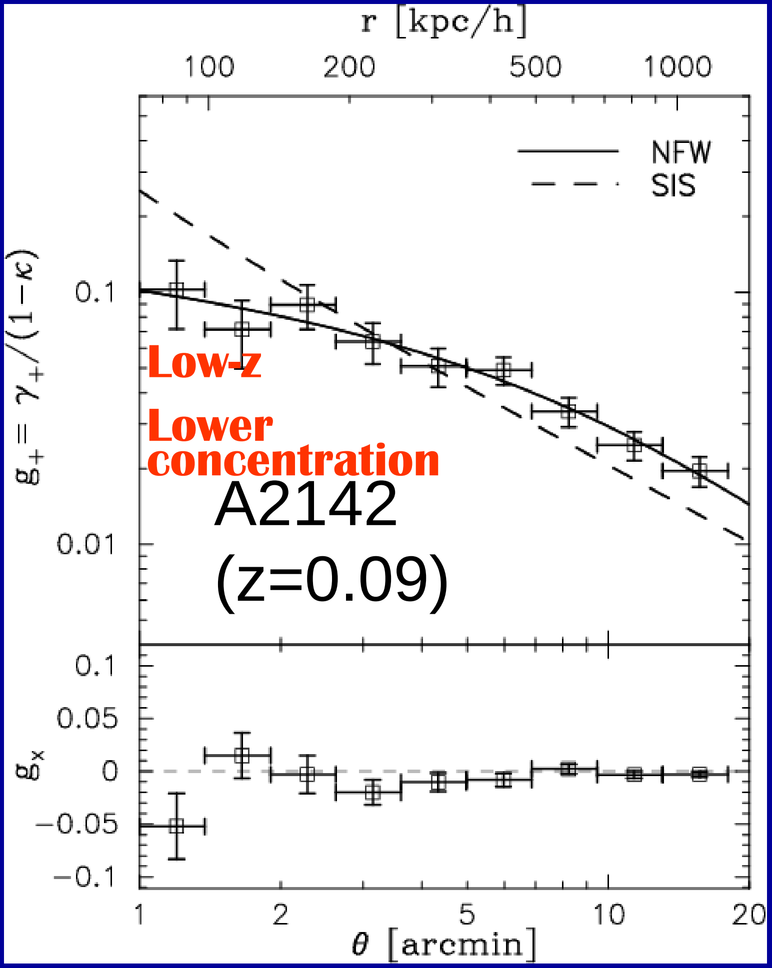

Umetsu, Birkinshaw, Liu+ 09, ApJ

Full Lensing Analysis: Weak + Strong Lensing

Galaxy cluster: CL0024+1654 (z=0.395)

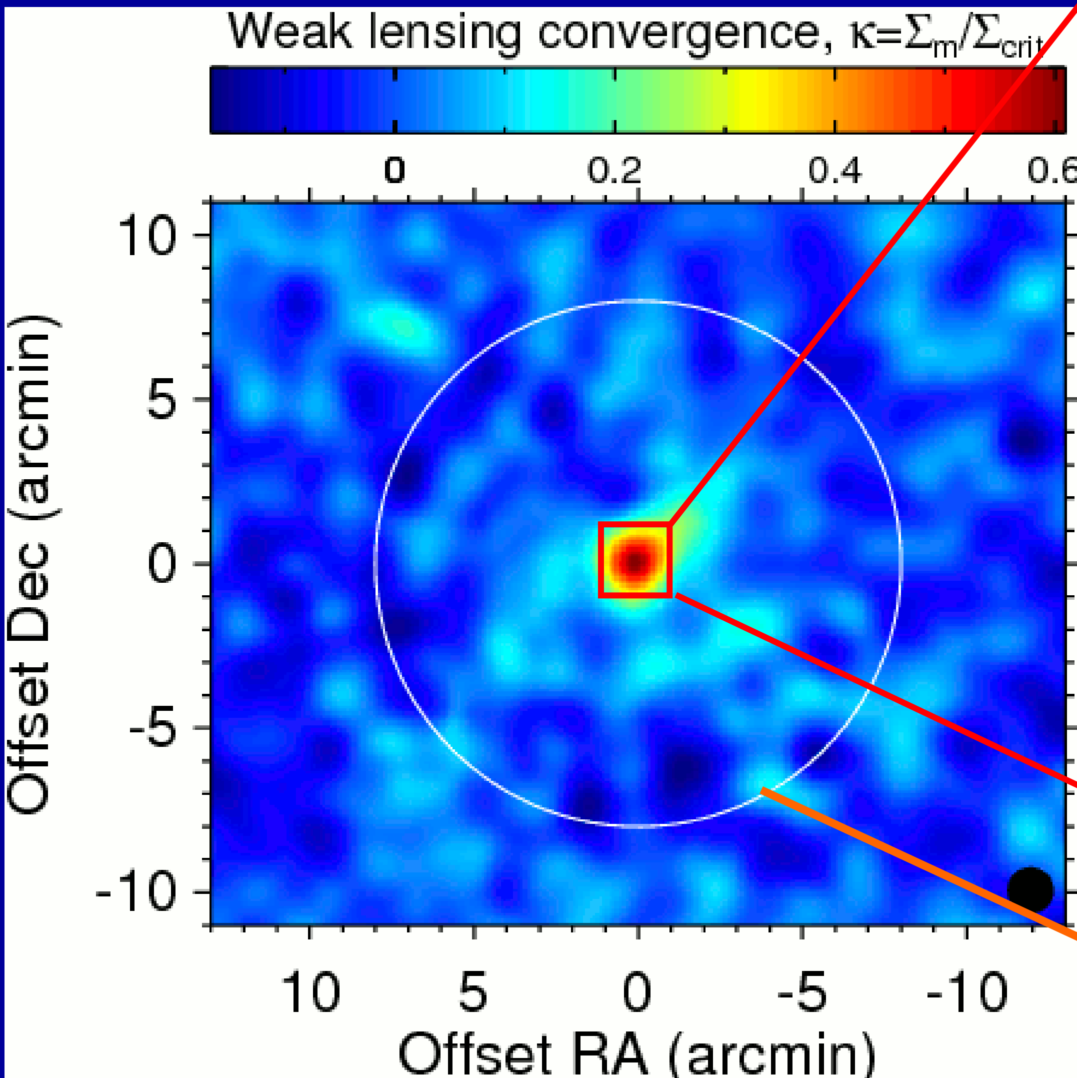

HST/ACS (2’x2’ region)

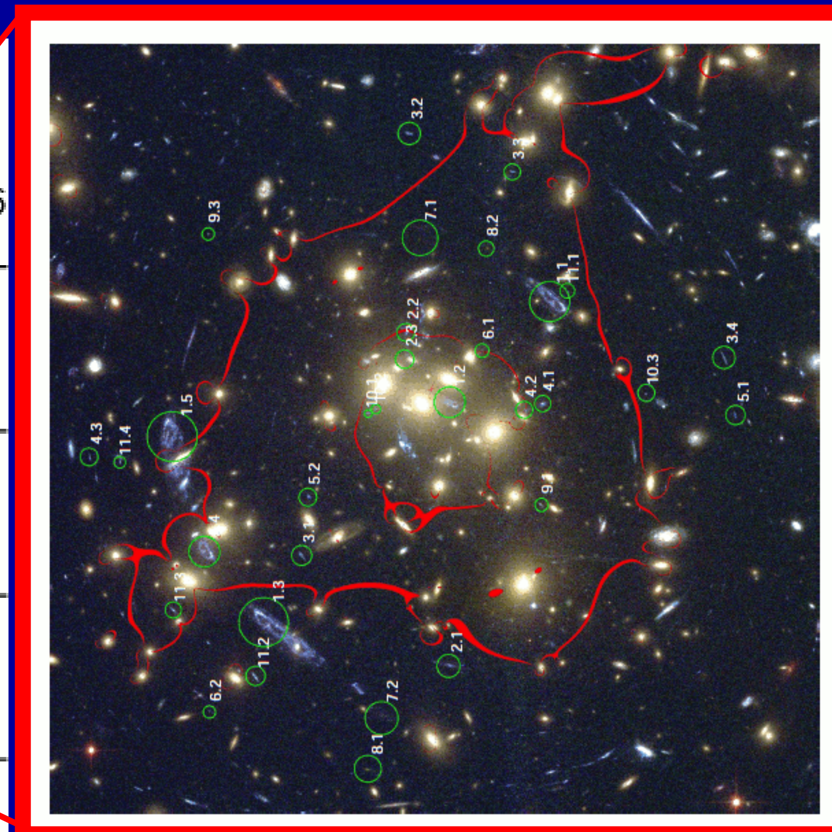

SUBARU/Suprime-Cam

R_{vir}=~ 1.8Mpc/h (~8 arcmin)

Umetsu et al. 2010

Equilibrium DM Density Profiles (contd.)

Combining Weak and Strong lensing data

→ Probing the mass density profile from 10kpc/h to 2000kpc/h

Results for Abell 1689 (z=0.183) and CL0024+1654 (z=0.395)

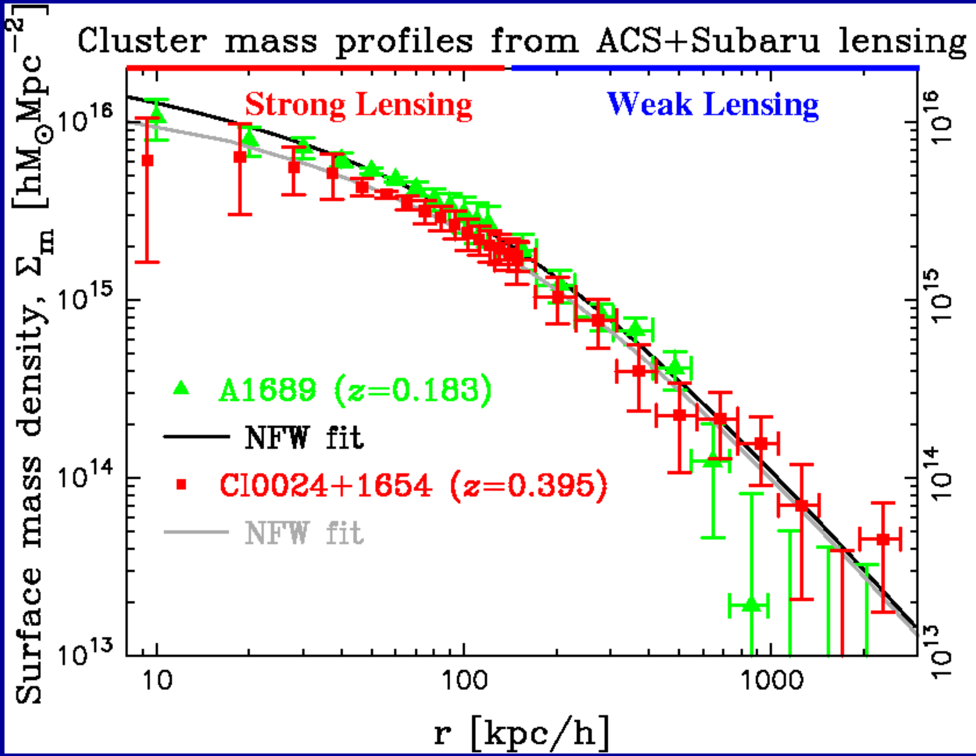

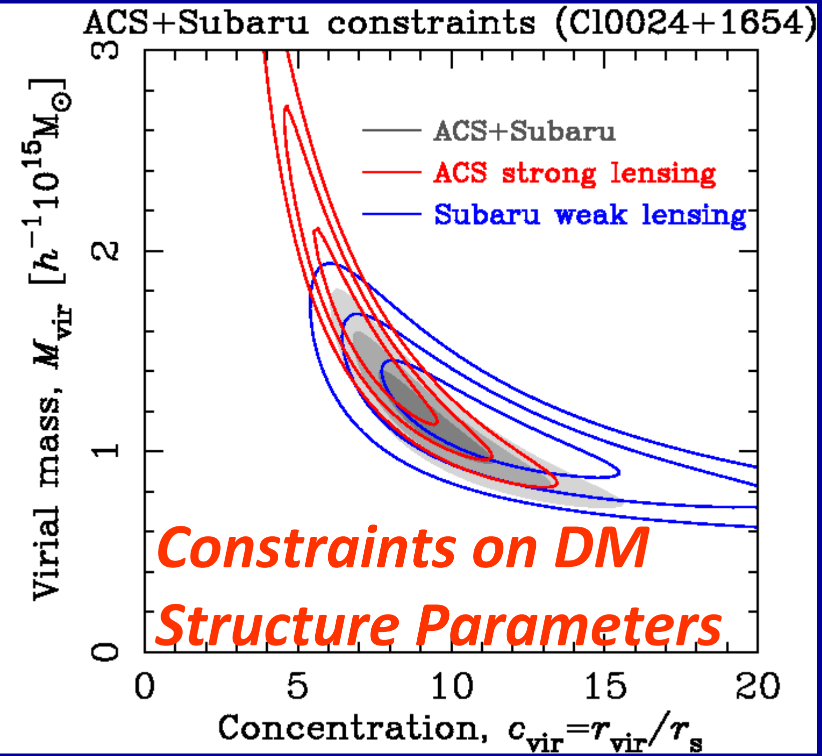

Umetsu & Broadhurst 2008, ApJ, 684, 177 (A1689)

Umetsu et al. 2010, arXiv:0908.0069 (CL0024+1654)

Stacked Cluster Weak Lensing Analysis

Stacking cluster WL distortion profiles from Subaru data

→ less sensitive to substructures/asphericity of individual clusters

$M<6e14M_{sun}/h$ **$M>6e14M_{sun}/h$**

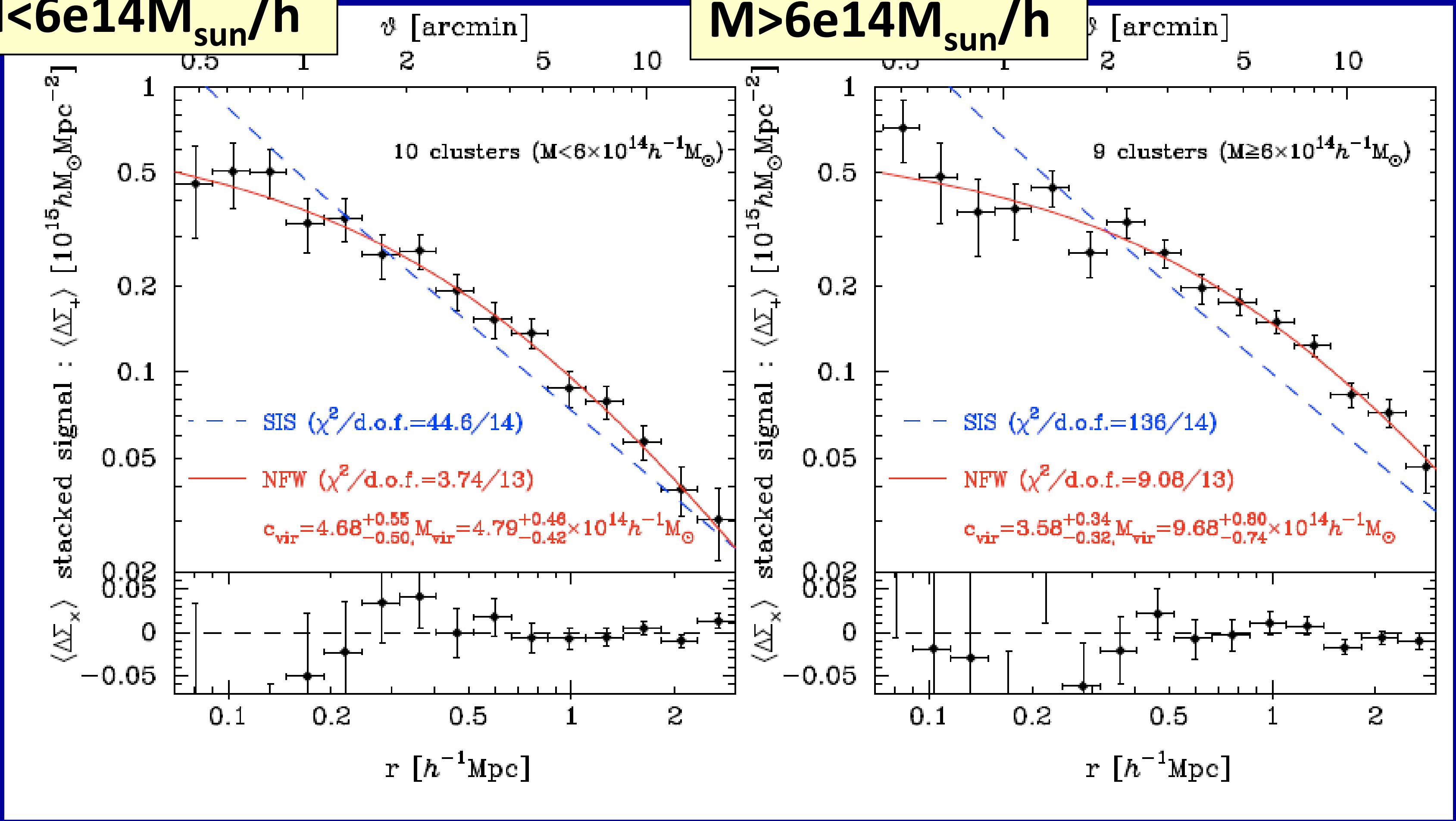

SIS rejected @6 and 11 σ levels (Okabe,Takada,Umetsu+ 10, arXiv:0903.1103)

3.3 Magnification Bias (Count Depletion)

Magnification bias: Lensing-induced fluctuations in the background density field (Broadhurst, Taylor, & Peacock 1995)

$$\delta n(\boldsymbol{\theta}) / n_0 \approx -2(1-2.5\alpha)\kappa(\boldsymbol{\theta})$$

with unlensed counts of background galaxies $n_0(<m) \propto 10^{\alpha m}$

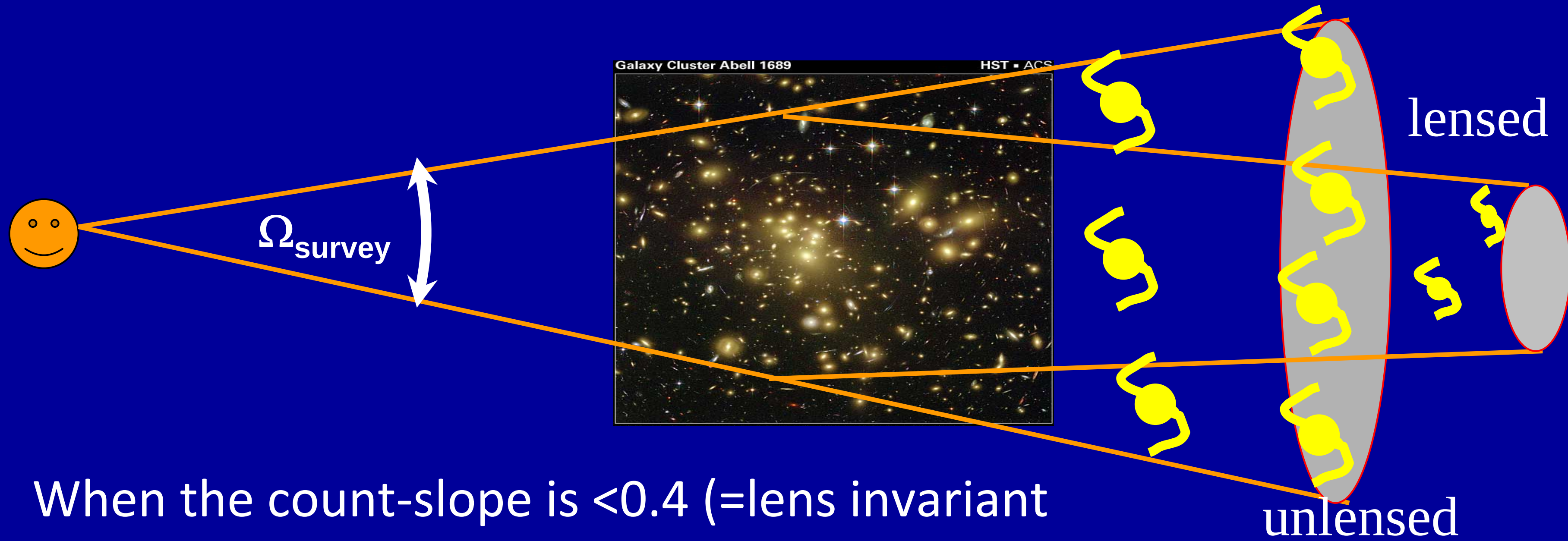

When the count-slope is <0.4 (=lens invariant slope), a net deficit is expected.

Cluster Depletion Profile in CL0024

Count depletion of "red" galaxies in CL0024

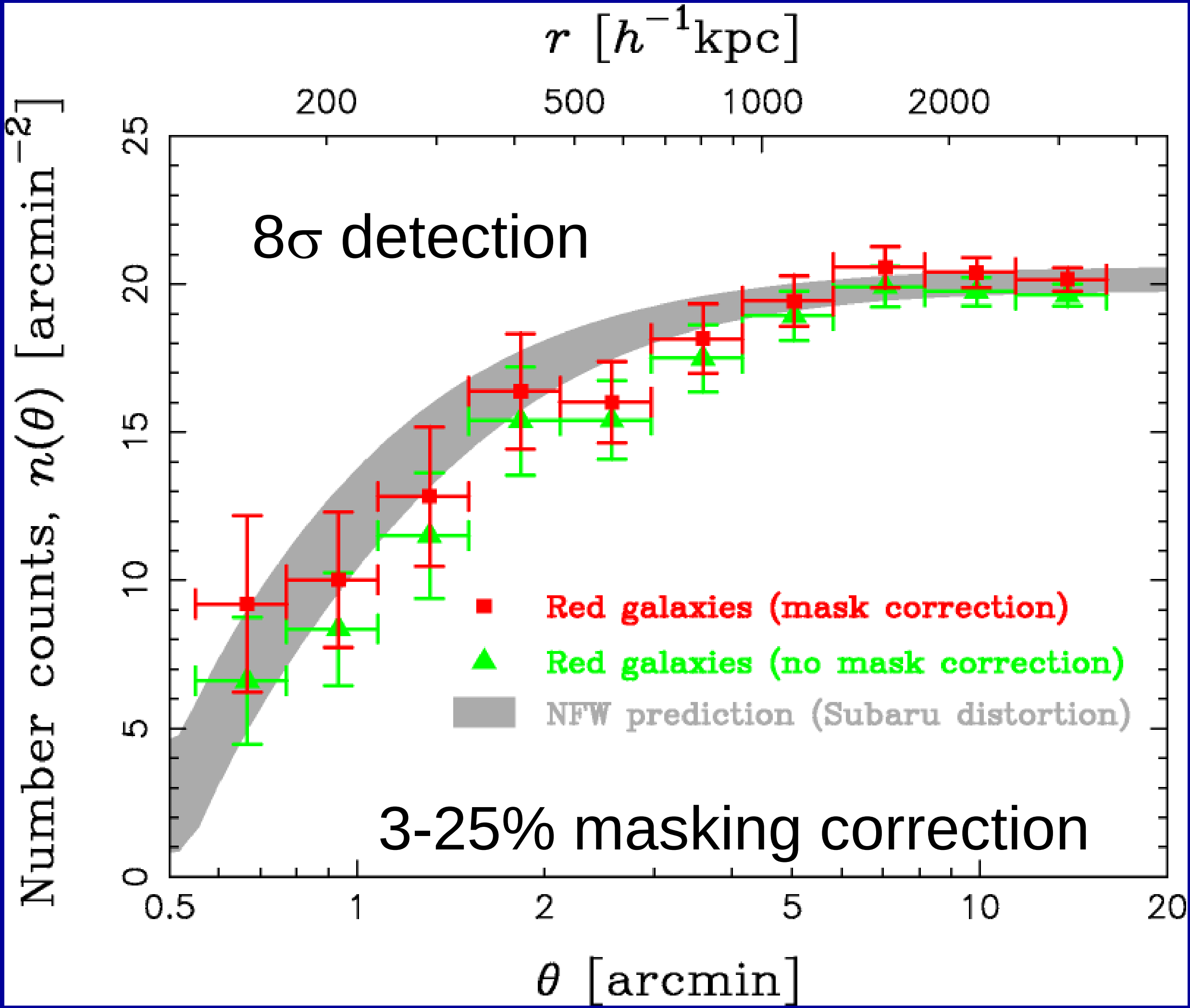

Distortion of "blue+red" sample

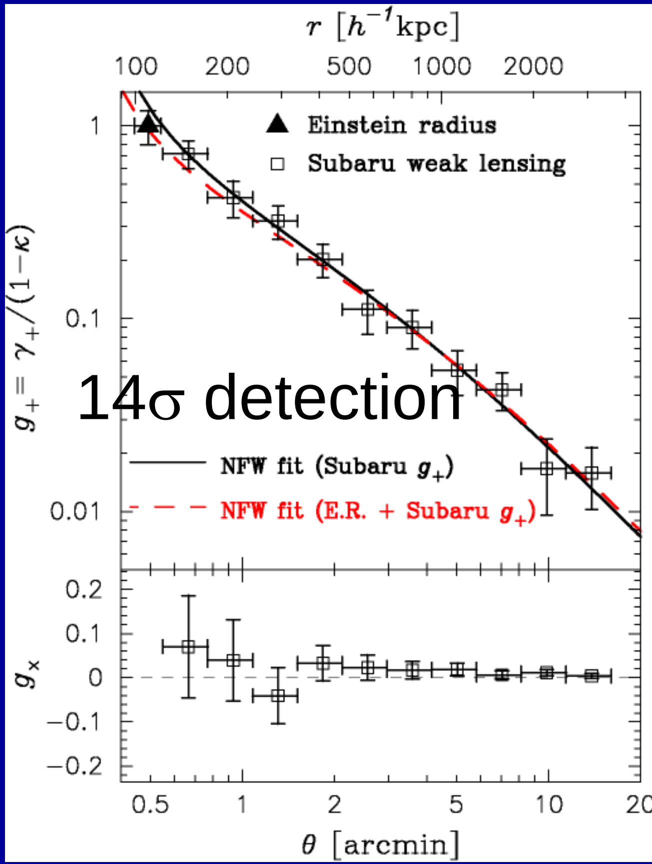

Umetsu et al. 2010, arXiv:0908.0069

Count Depletion in Other Clusters

Lens distortion (left) vs. depletion (right) in high-mass clusters

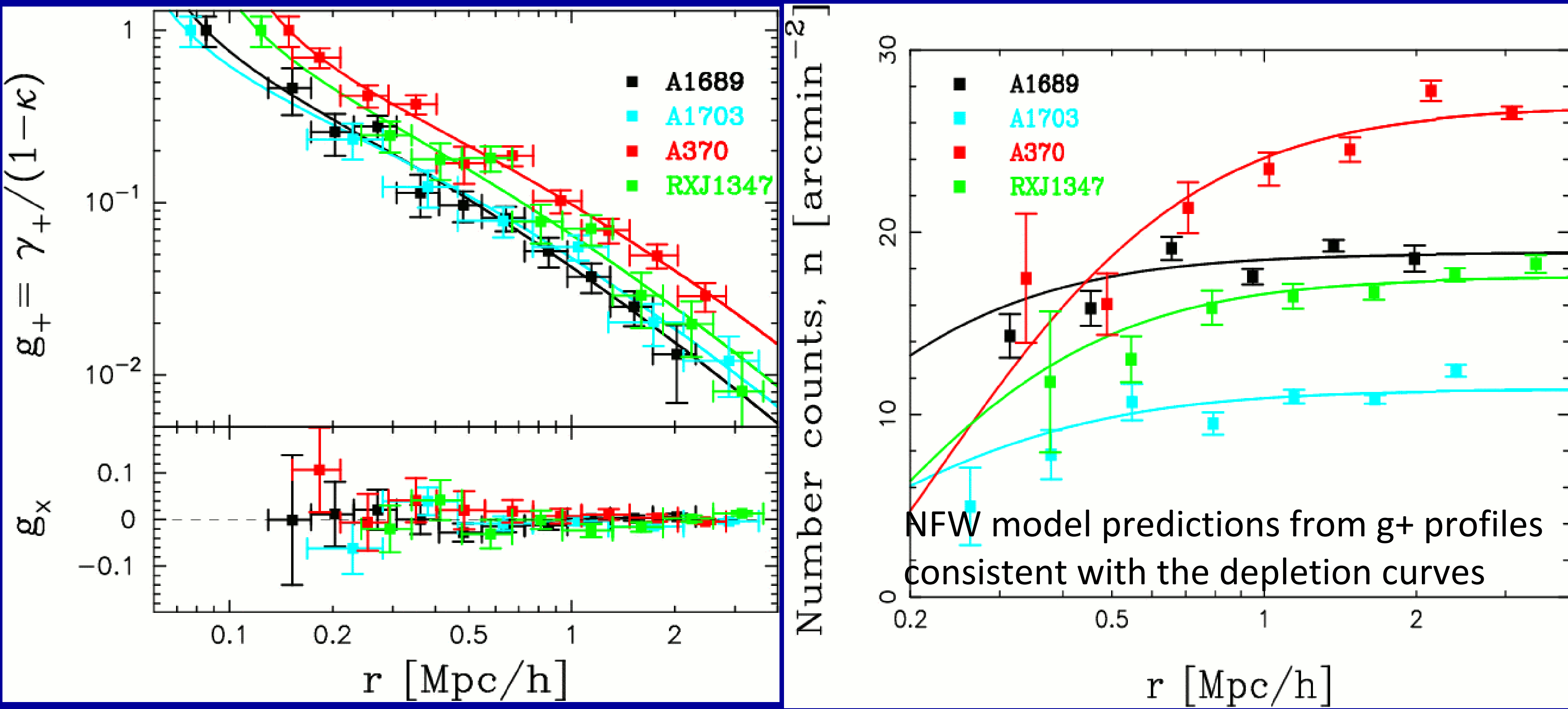

Observed curves are similar in form, well described by CDM-consistent NFW profiles

Broadhurst, Umetsu, Medezinski+ 2008, ApJ, 685, L9

Other Interesting Topics on Cluster Lensing

- **Weak Lensing Flexion and HOLICs**
  - Next higher-order weak lensing distortions, responsible for weakly-skewed arc-like images, or *arclets* (Goldberg & Bacon 2005; Bacon et al. 2006)
  - Can be used to measure directly the mass of giant elliptical galaxies
  - Moment-based HOLICs (Higher Order Lensing Image Characteristics) formalism given by Okura, Umetsu, Futamase 2007, 2008
- **Cluster-Galaxy Galaxy Lensing**
  - Stack the tangential distortion signal around cluster member galaxies to measure the averaged mass profile of cluster galaxies (e.g., Natarajan et al. 2009).
  - Can be used to study the cluster galaxy masses as a function of cluster environments, which may reveal imprints of cluster internal dynamics, such as tidal stripping
- **Weak Lensing Dilution**
  - Use dilution of the weak lensing signal to measure the number fraction of cluster galaxies, which can be then used to measure the cluster luminosity and the cluster luminosity function (Medezinski, Broadhurst, Umetsu et al. 2007, 2010)

4. The Y.T. Lee AMiBA Project

Academia Sinica IAA

National Taiwan University, Physics and Electrical-Engineering Dept.

4.1 CMB Interferometers

CMB vs. Interferometer

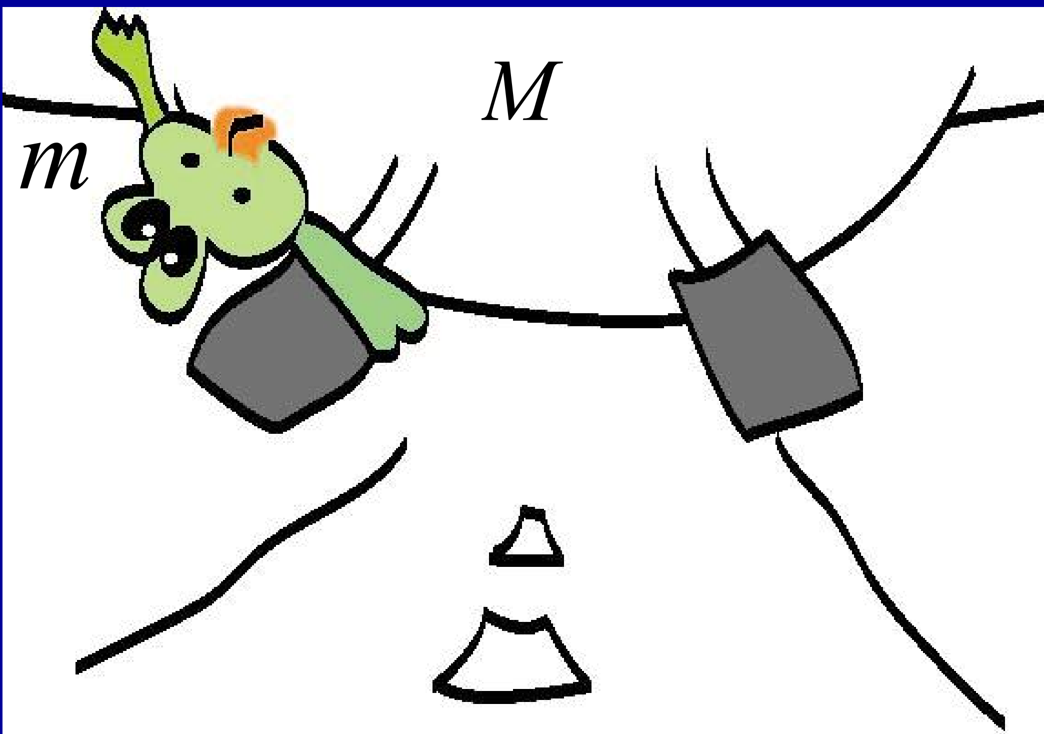

Interferometer measures directly m

Credit: Prof. Atsuto Suzuki, Tohoku U.

Figure by Prof. Makoto Hattori

How to weigh a frog that is attached to a Jumbo-Jet?

Single dish observations compare two measurements:

$$(M + m) - M' = m$$

M : weight of Jumbo with the frog

M' : weight of Jumbo without a frog

Measurement of CMB anisotropy: $\frac{m}{M'} < 10^{-5}$

Observable: Complex Visibility, V(u,v)

E-field measured by a pair of receivers, being cross-correlated to form a complex visibility

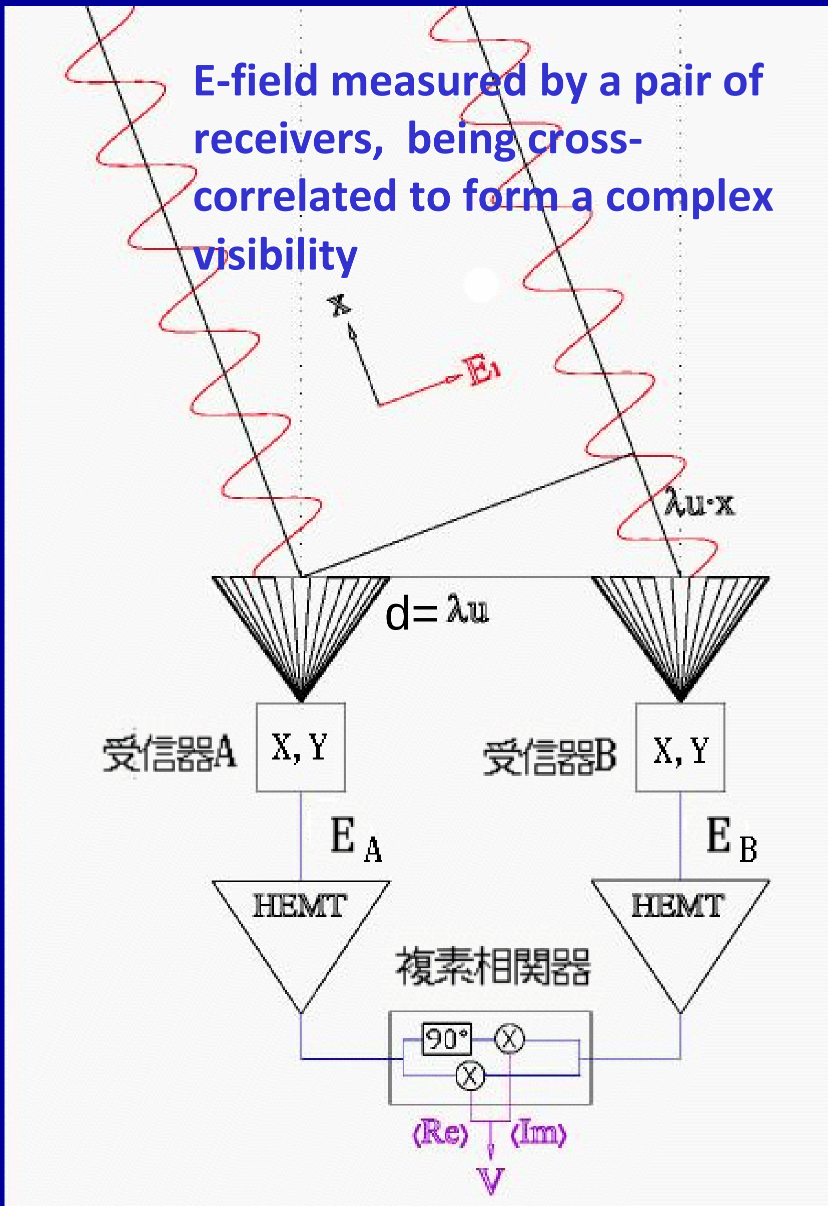

$$V(\vec{u}) = \int d^2x\, A(\vec{x}) I(\vec{x}) \exp[2\pi\, i \vec{u}\cdot\vec{x}]$$

$$\vec{u} = \vec{d}/\lambda \quad \text{baseline vector}$$

I(x) : intensity map on the sky

A(x) : antenna primary beam pattern

Visibility is Fourier Transform of intensity pattern I(x) attenuated by A(x)

$$V(\vec{u}) = \mathbf{FT}[A(\vec{x}) I(\vec{x})]$$

Angular power spectrum directly measured by interferometer!!

$$C_l \,\big|_{l=2\pi u} \approx \left\langle V(\vec{u}) V^*(\vec{u}) \right\rangle$$

Fringes

Moon fringes measured in drift-scanning observations with the 2-element AMiBA prototype (2002-2004)

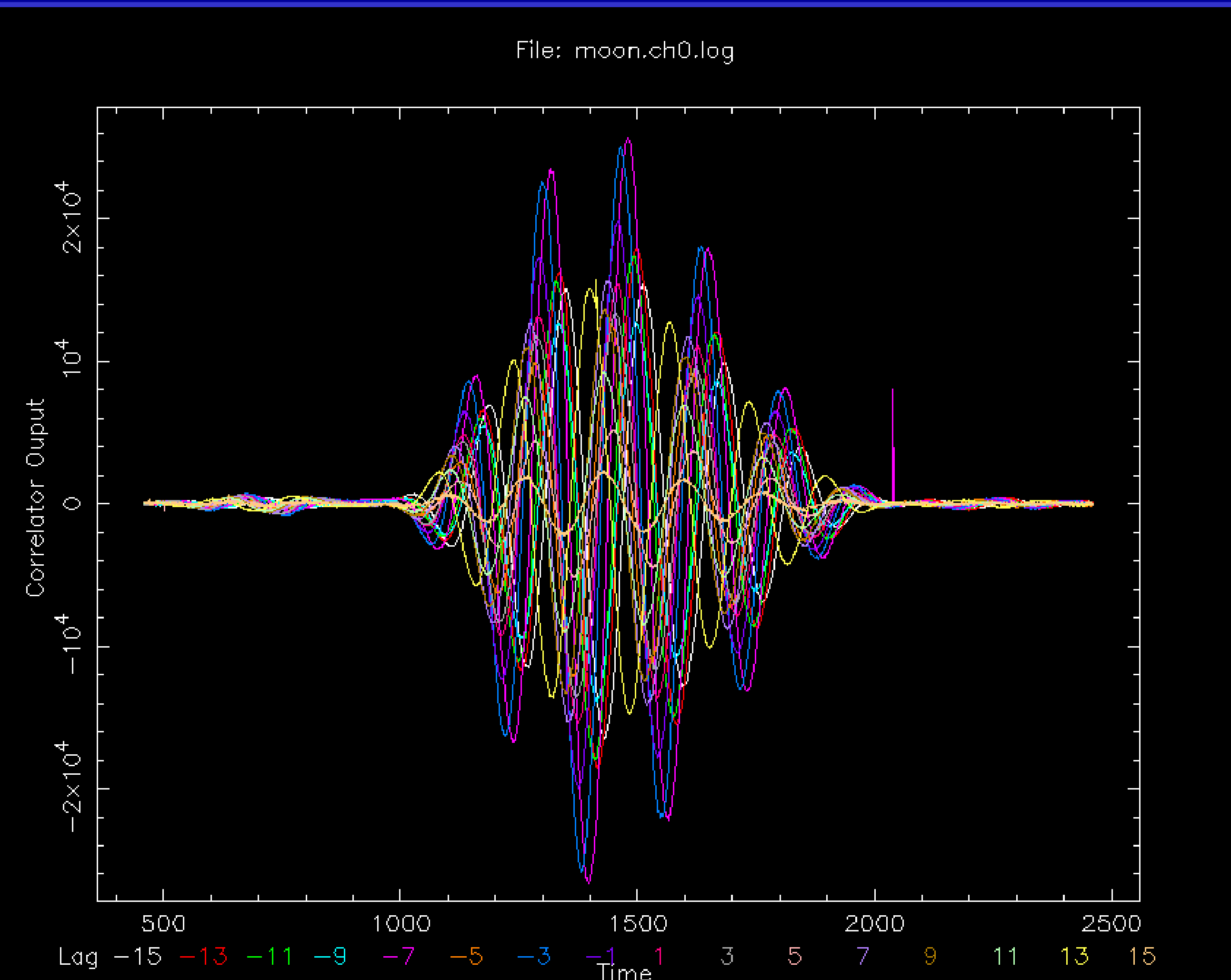

transit

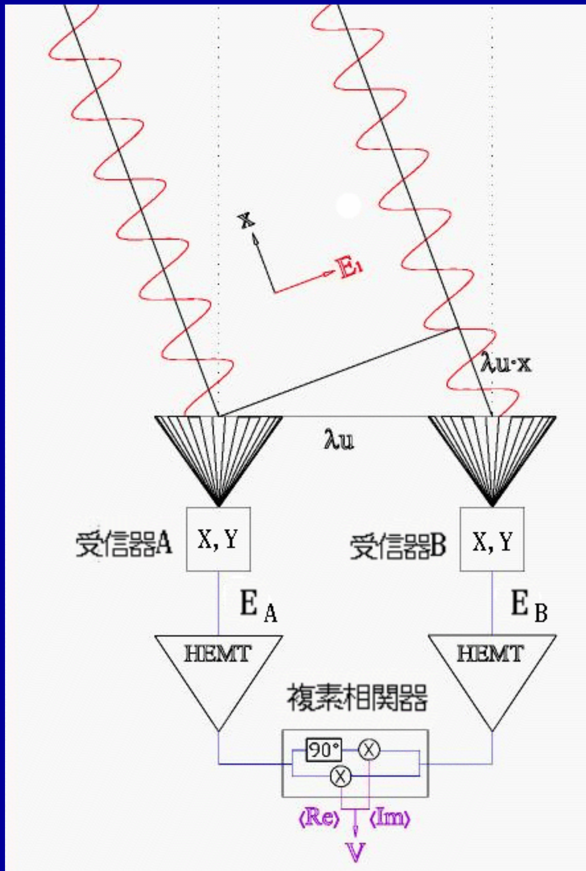

CMB Interferometers

- Typical angular sizes ~ 1degree – 10 arcmin
  → small antennas, and/or, low frequency (10-100GHz)
- CMB anisotropy = diffuse, weak signal (10-100μK)
  → close-packed, or compact array to maximize sensitivity
- Observing strategies, different from traditional ones
  e.g., NO geometrical delay to creat fringes while tracking

$$\Delta\theta = \frac{1}{\Delta u} \approx 20' \left(\frac{d}{60\mathrm{cm}}\right)^{-1} \left(\frac{\lambda}{3\mathrm{mm}}\right)$$

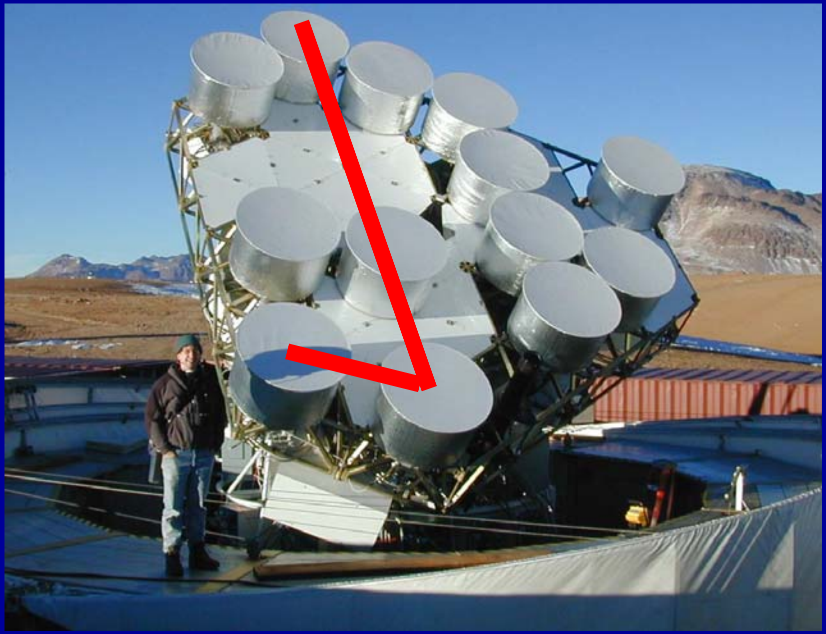

CBI @ 26-36 GHz, 13 elements, Chile (1999~)

DASI @ 26-36 GHz, 13 elements, South Pole (1999~)

Uniform UV-Coverage

Traditional interferometer
[2-axes: Azimuth, Elevation]

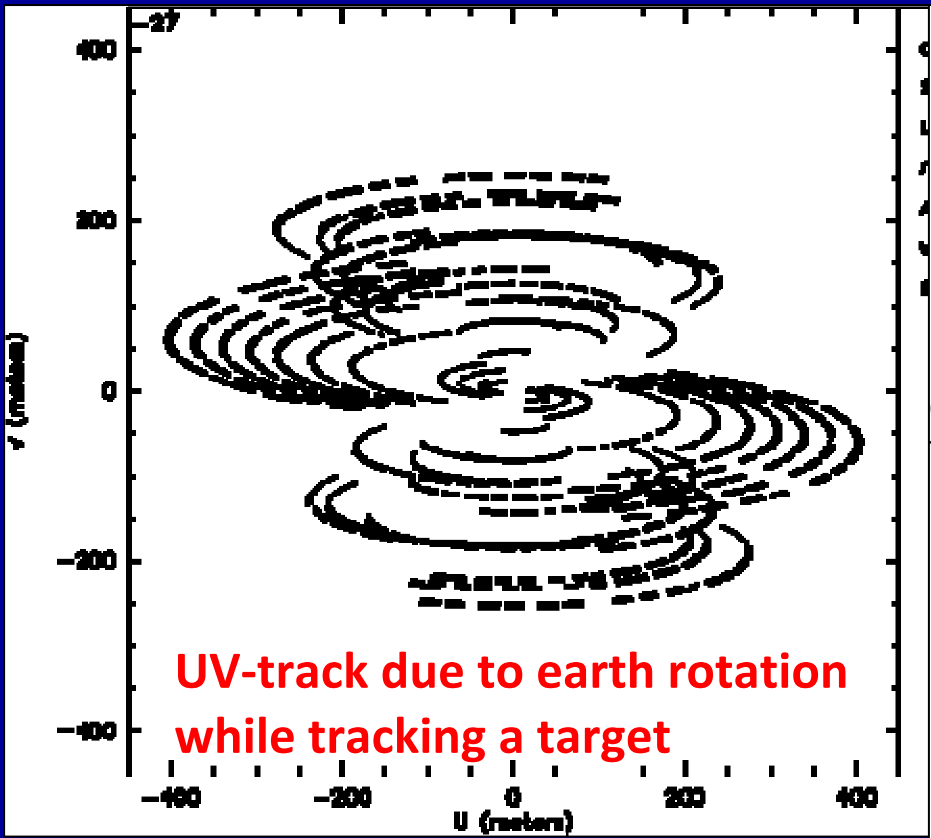

AMiBA with active platform rotations
[3-rotation DoF: Az, El, Pol]

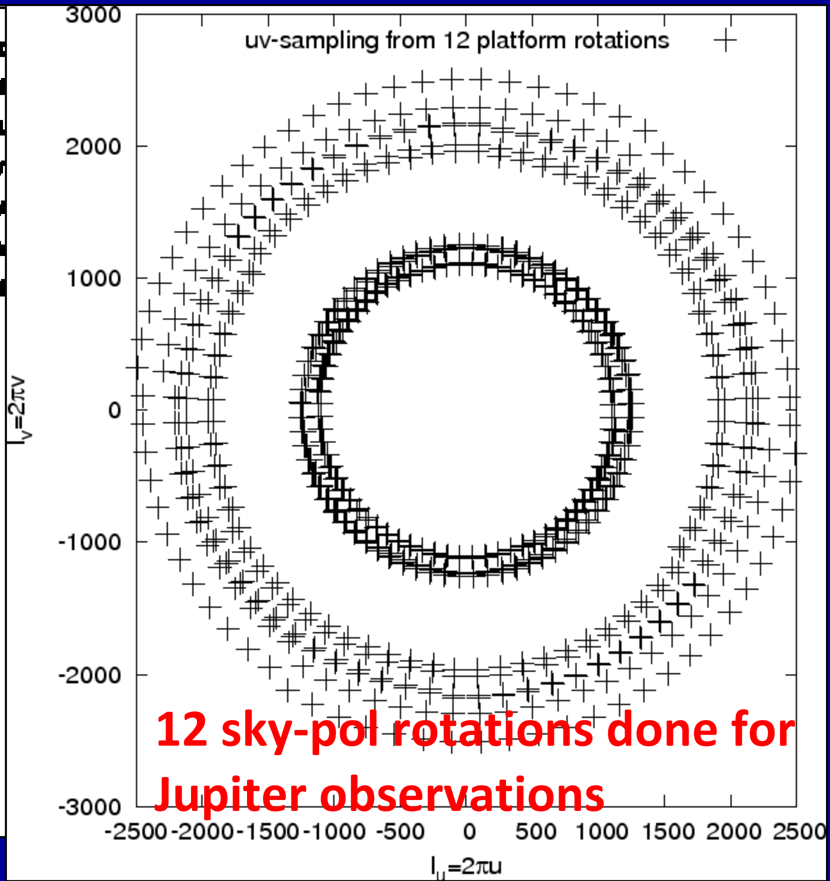

Synthesized beam (PSF) is an **Inverse FT** of the UV-sampling function:

$$B(\vec{x}) = \mathbf{FT}^{-1}[S(\vec{u})]$$

4.2 The AMiBA Project

Science Goal (I)

Power Spectra C_l of CMB Anisotropies

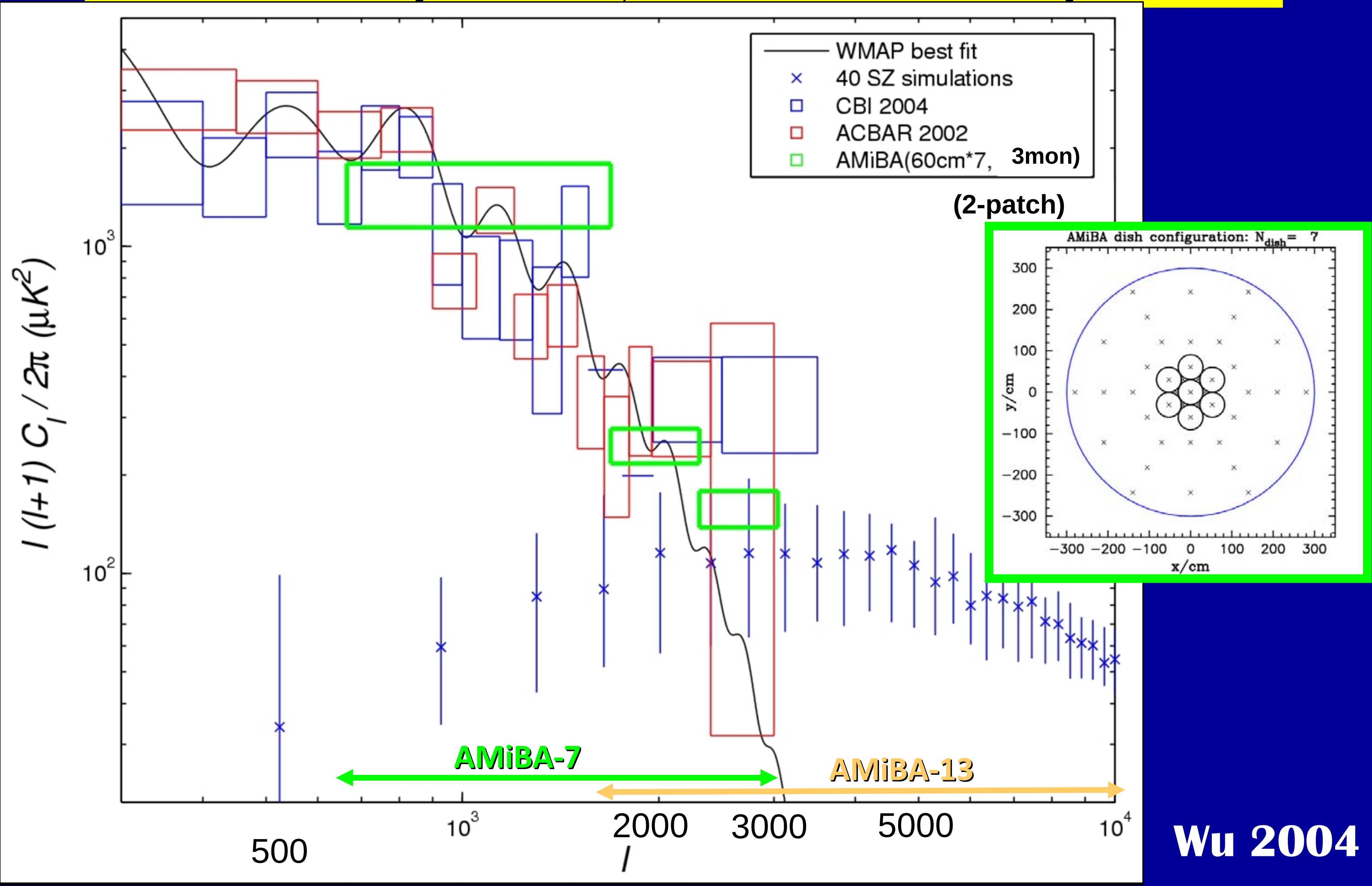

Wu 2004

Science Goal (II)

Study and Search for Clusters via SZE

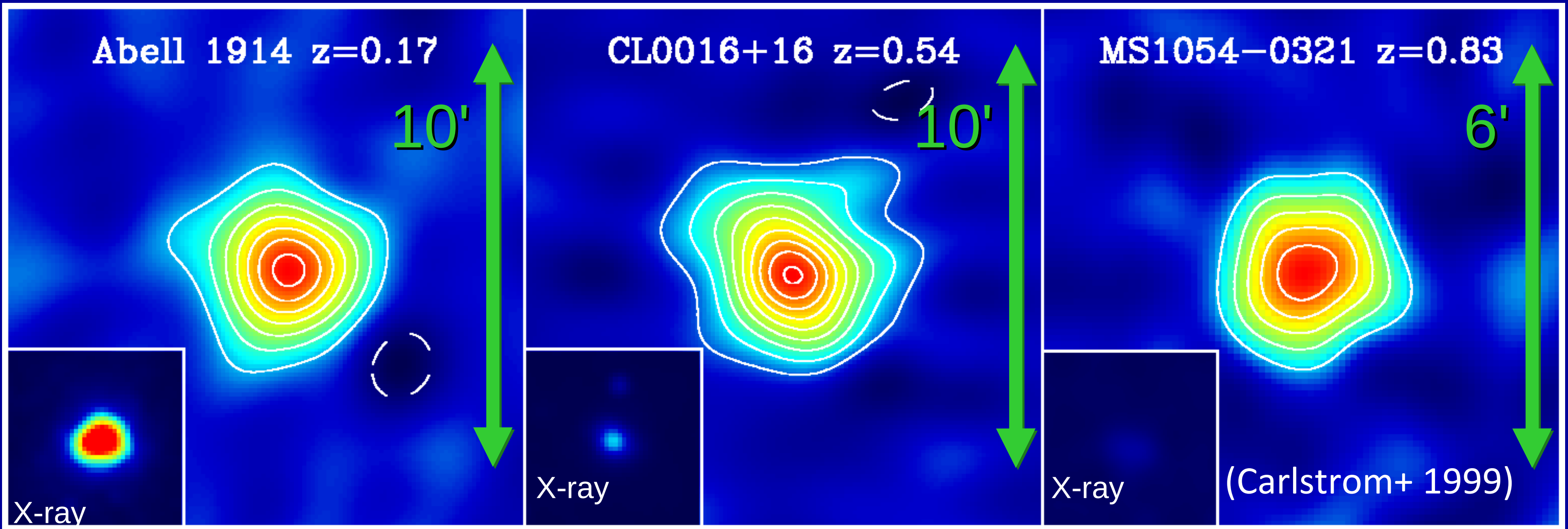

Brightness of Sunyaev-Zel'dovich effects (SZE), z-independent:

Free from cosmological brightness dimming, $(D_A / D_L)^2 \propto (1+z)^{-4}$

Signal strength of thermal SZE

$$y \equiv \int_0^{\lambda_{\rm LSS}} d\tau \, \frac{k_{\rm B}(T_{\rm e} - T_{\rm CMB})}{m_{\rm e} c^2} \approx \int \frac{k_{\rm B} T_{\rm e}}{m_{\rm e} c^2} \sigma_{\rm T} n_{\rm e} dl \propto \int dl \, P_{\rm e}$$

What we seek for is a 10-100 μK weak signal!!

What is the AMiBA Project?

AMiBA is:

– a platform-mounted *interferometer* operating at 3mm, specifically designed to study the structure of CMB at l=800-8000 (20 to 2 arc-minutes)
  - The 7-element AMiBA (AMiBA-7) focused on SZE observations for galaxy cluster physics and cosmology
  - 9 papers published/accepted in ApJ, 2009-2010; 4 more papers submitted to ApJ

– the first major astronomical project designed, constructed, operated, and led by Taiwan

– *so far the first & only* CMB/SZE telescope for Asia

– *one of few SZE instruments operating at 3mm* (where foreground/CMB contamination is minimized) with published scientific results: cf. SPT bolometer array, SZA interferometer at 1cm (1’-10’) and 3mm (<1’)

Probing Arcminute-Scale CMB Structures

Input CMB+SZE sky @ 94GHz

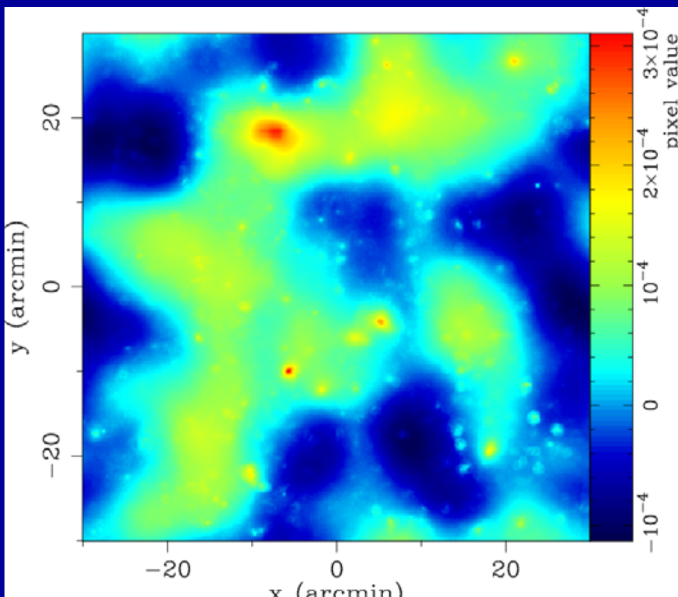

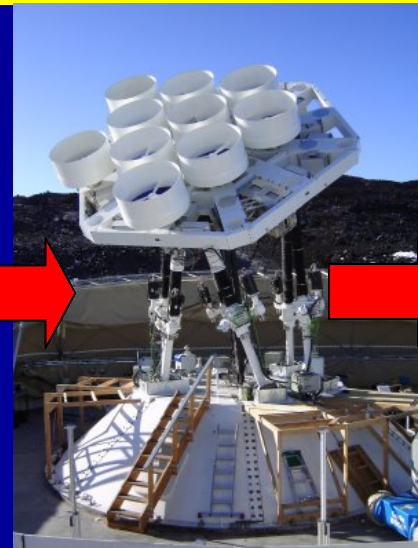

2' FWHM beam

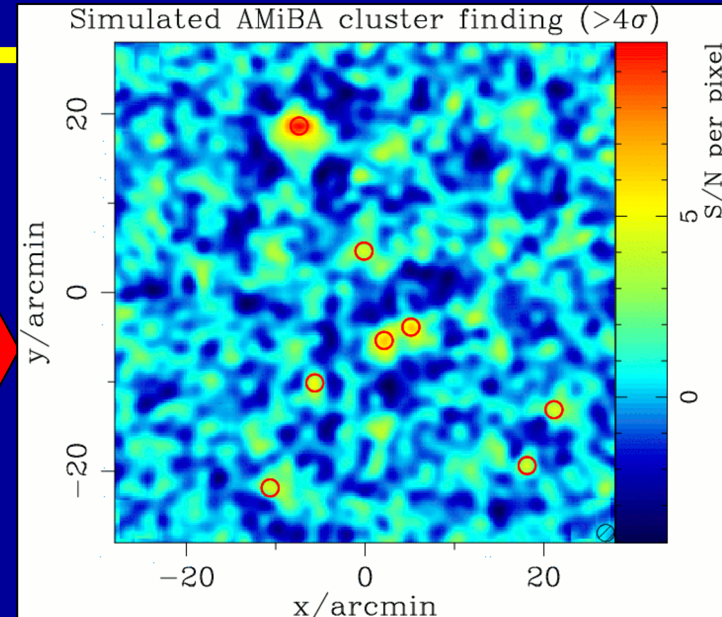

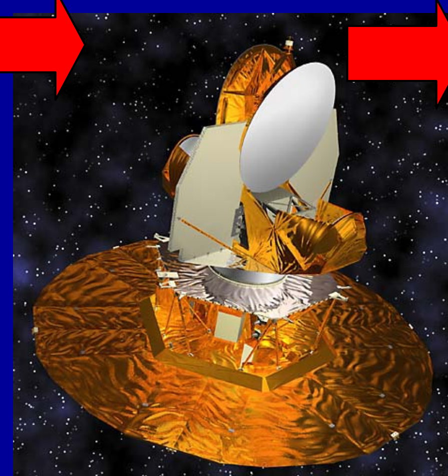

14' FWHM beam

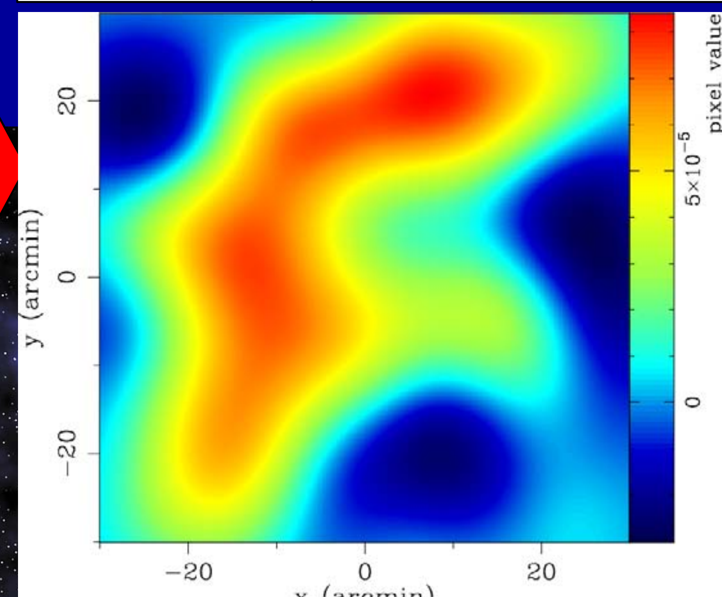

Umetsu, Chiueh, Lin+ 2004

AMiBA will target angular scales smaller than WMAP to study cluster-sized structures (R~1Mpc) via the SZ Effects.

AMiBA-7 Science Highlights

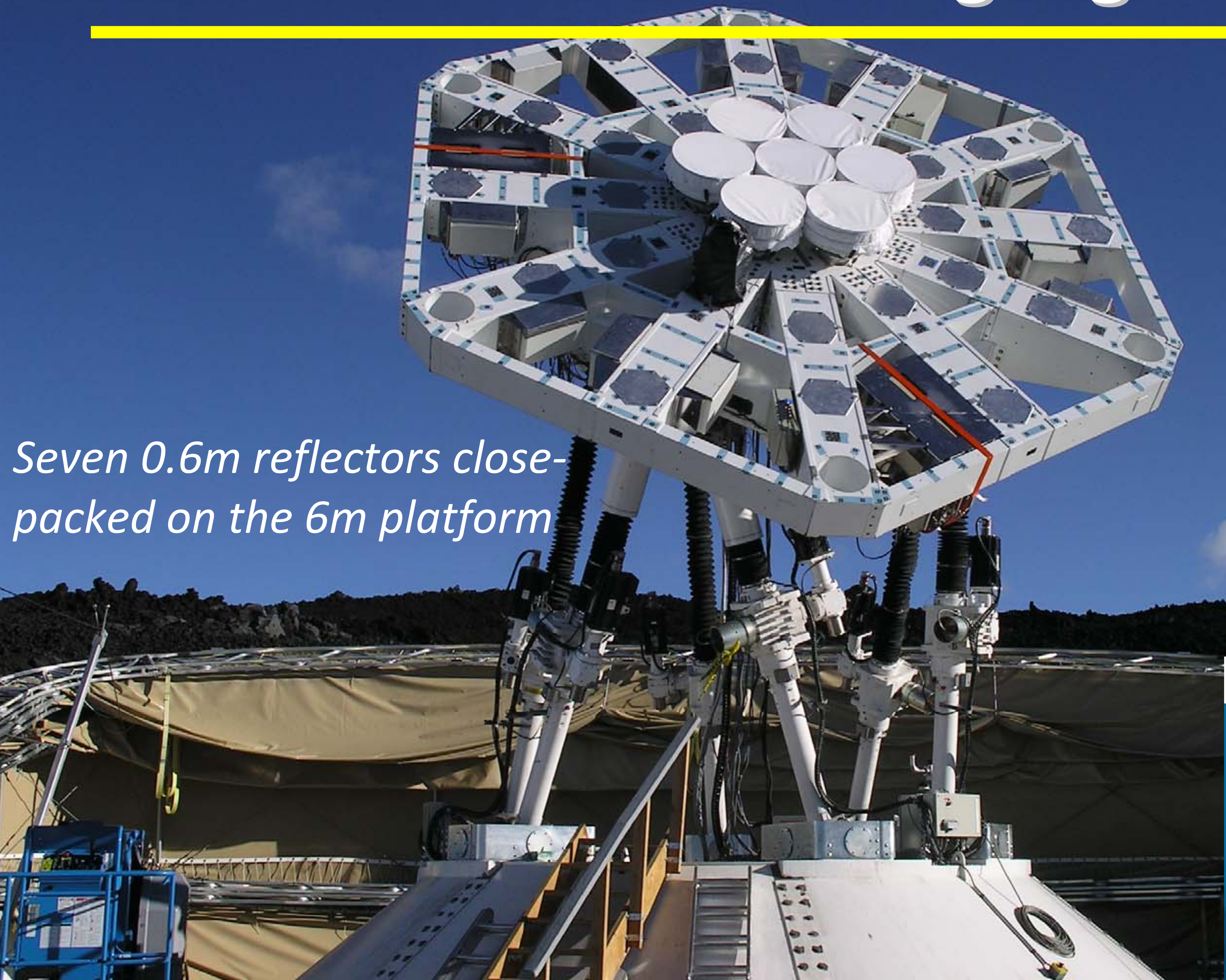

Seven 0.6m reflectors close-packed on the 6m platform

AMiBA-7 SZE Maps

J.H. Proty Wu et al. 2009, ApJ, 694, 1619

Obtained AMiBA images of SZE decrement towards 6 Abell clusters in 2007

CLEANed images (z=0.1-0.3)

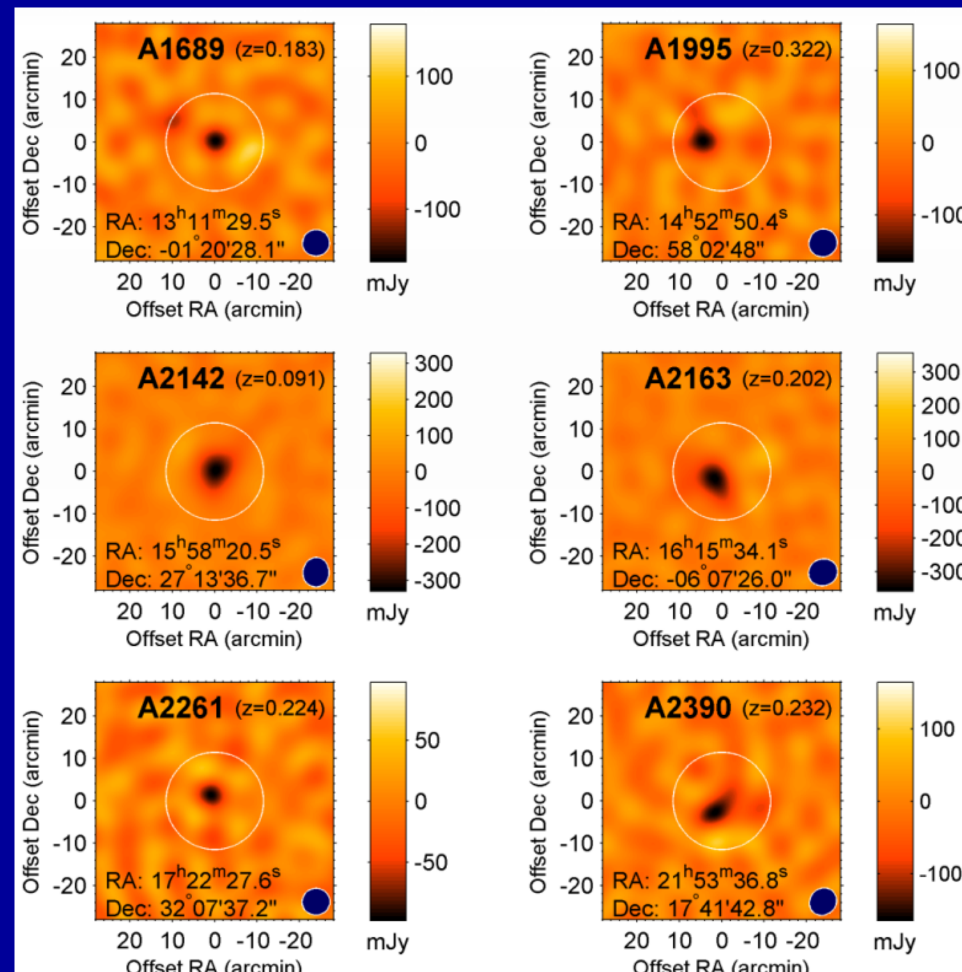

Power of AMiBA/SZE for Cluster Physics

Paul T.P. Ho et al. 2009, ApJ, 694, 1610

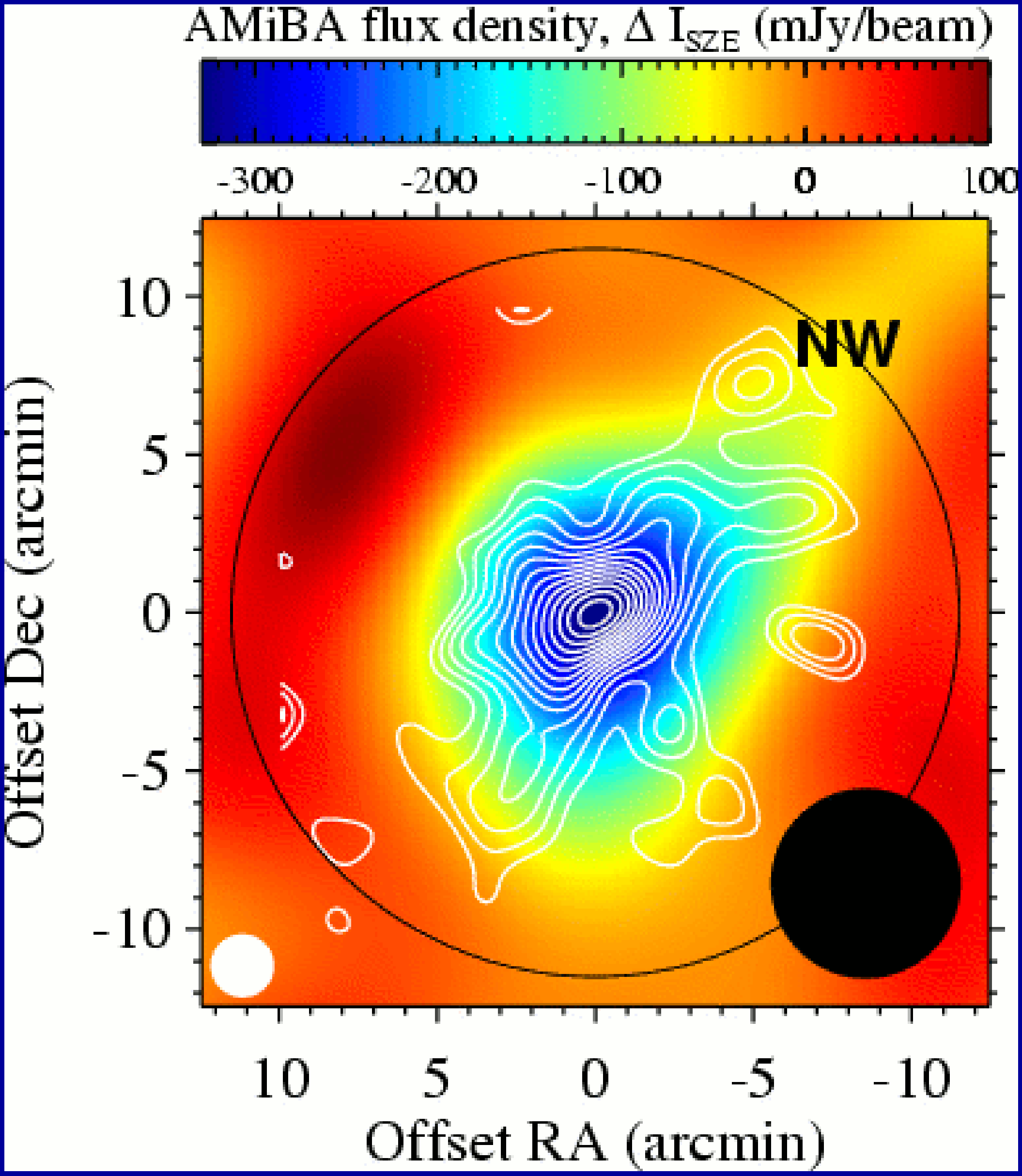

A2142 – merging cluster with X-ray cold fronts

- **Large scale** NW-SE structure consistent between AMiBA SZE (color-coded) and Subaru weak lensing (white contours)
- **Extended SZE excess** associated with the NW mass clump is detected, which may be indicating a pressure increase in the IC gas.
- **Power of AMiBA SZE** to probe the ICM in low-density outskirts where X-ray emission is not sensitive.
- **AMiBA-13** will sharpen the SZE map, probing the merger physics in clusters.

Cluster Gas Fractions from Subaru/S-Cam WL + AMiBA SZE

First "Lensing+SZE" based cluster gas fraction measurement out to large radii (r_{200}), without assuming hydrostatic equilibrium

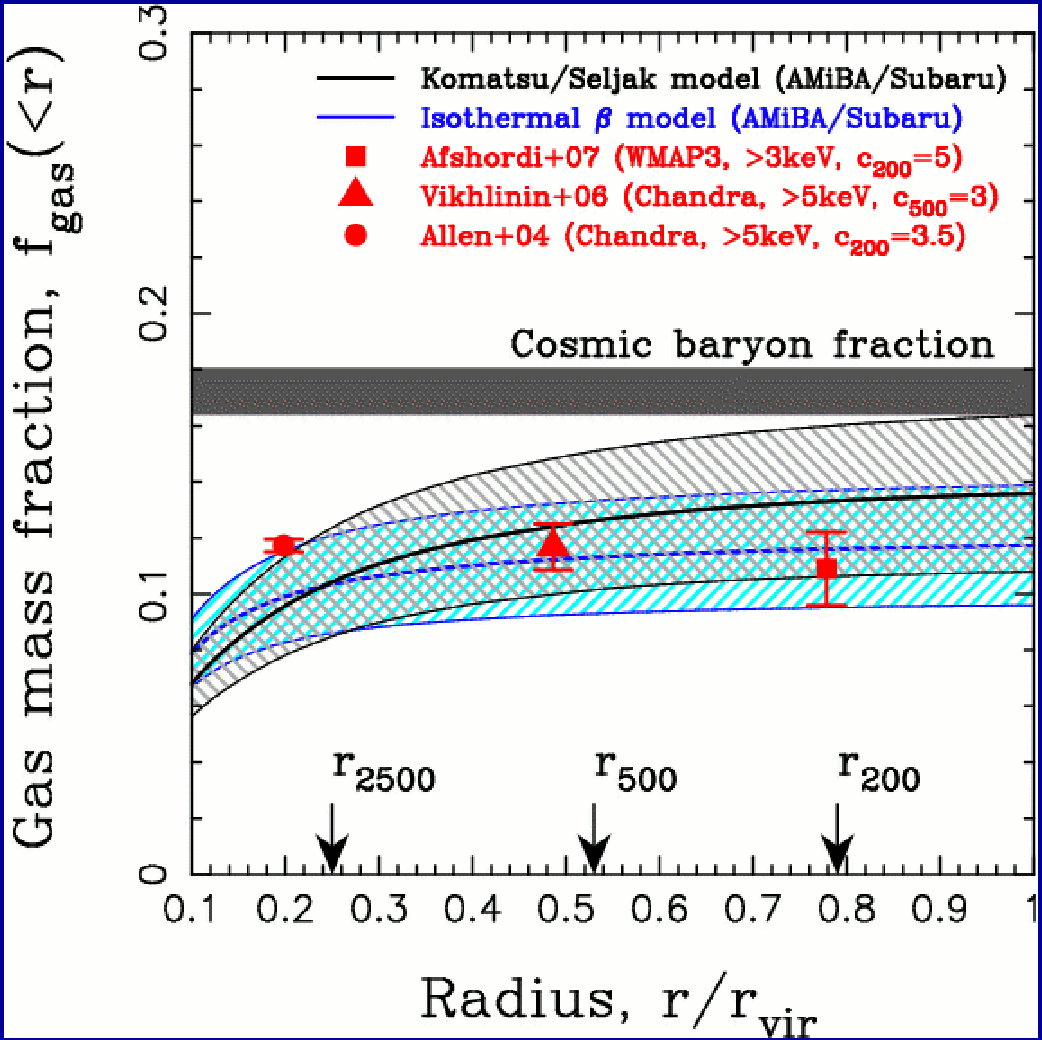

$$\langle f_{gas}(r_{200})\rangle \equiv \frac{M_{gas}(r_{200})}{M_{tot}(r_{200})} = 0.133 \pm 0.027$$
$$\leq \frac{\mathrm{B}}{\mathrm{DM}+\mathrm{B}} \equiv \langle f_b \rangle$$

$$\langle f_{gas}(r_{200})\rangle / \langle f_b \rangle = \left(\frac{\mathrm{Hot}}{\mathrm{Hot}+\mathrm{Cold}}\right)_{\mathrm{Baryons}} = 0.78 \pm 0.16$$
$$\text{with } \langle f_b \rangle = \Omega_b / \Omega_m = 0.171 \pm 0.009$$

- (22 +/- 16)% of the baryons are missing from the *hot plasma phase* in X-ray hot clusters >8keV
- ~5% can be accounted for by "cool" baryons (stars in galaxies, diffuse IC-light): cf. Gonzalez+05

Umetsu et al. 2010, ApJ, 694, 1643

SZE Observations with AMiBA-13

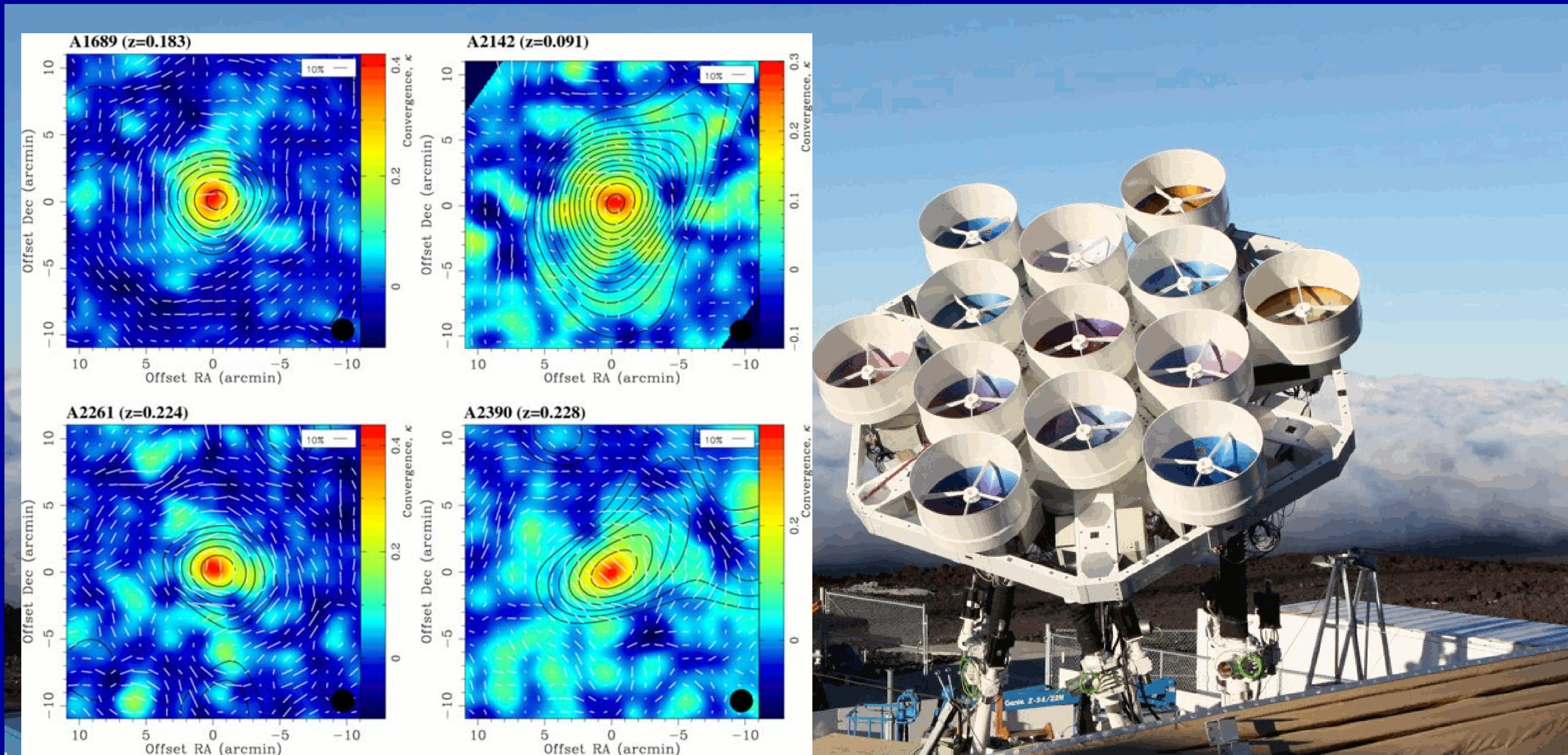

- 7-element AMiBA science operation completed (2007-2008): First resutls on SZE cluster sciences published in ApJ
- Science operation with the 13-element AMiBA has started.
- Coordinated Subaru weak lensing observations being conducted (March 2009 and 2010)

Summary

- Galaxy clusters, the largest bound astrophysical objects in the Universe, serve as astrophysical laboratories as well as cosmological probes.
- Gravitational Lensing offers the most direct route to the total mass distribution (dominated by invisible DM) in clusters, regardless of their physical/dynamical state or matter contents.
- Gravitational lensing thus provides an important basis for cluster studies via multi-wavelength observations , such as the internal dynamics of relaxed clusters, the dynamics of merging clusters, and the physical interplay between DM and ICM in forming clusters, etc.

Cluster Lensing: Strong/Weak Regimes

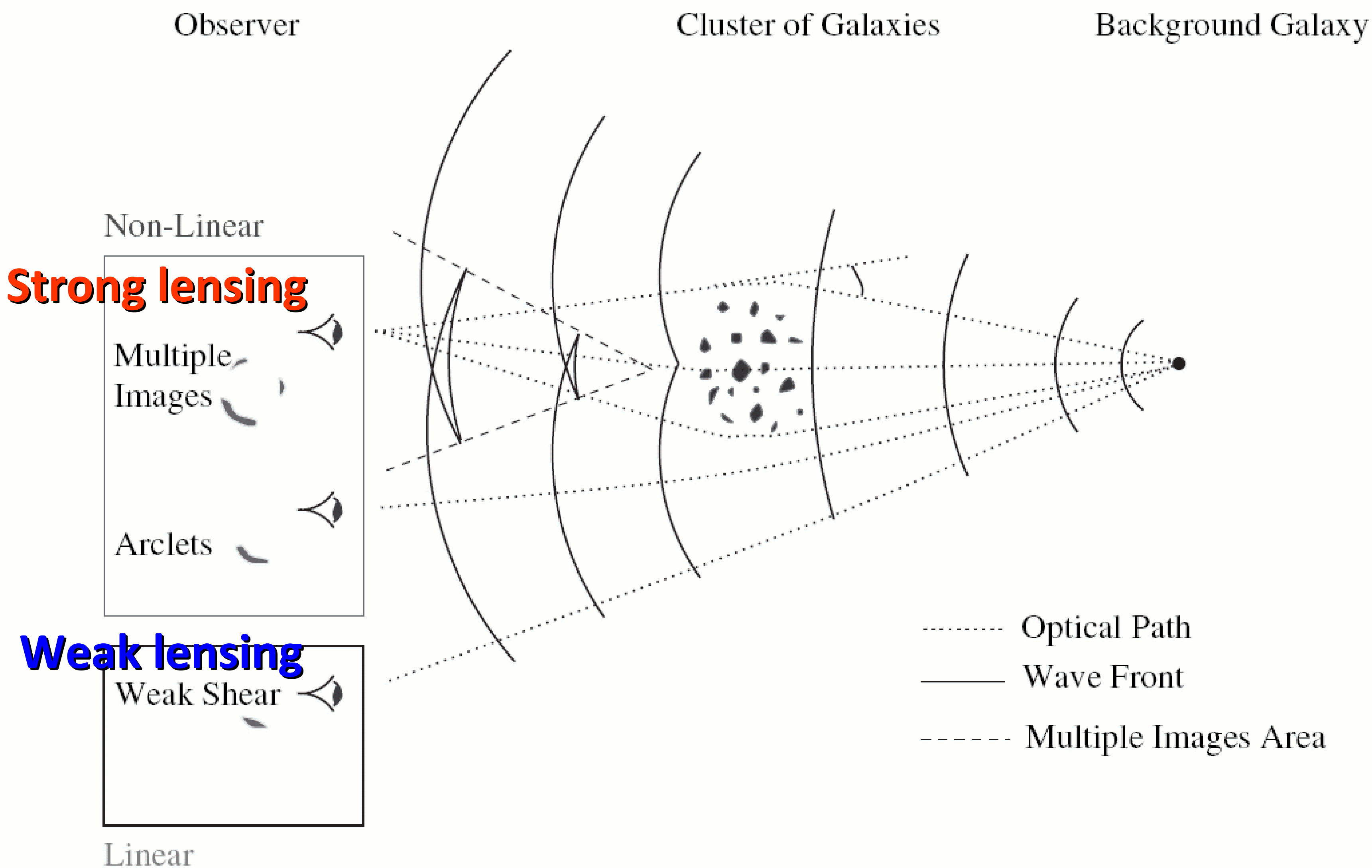

Lens Distortion + "Einstein Radius"

CL0024+1654 (z=0.395)

Constraints on DM Structure Parameters

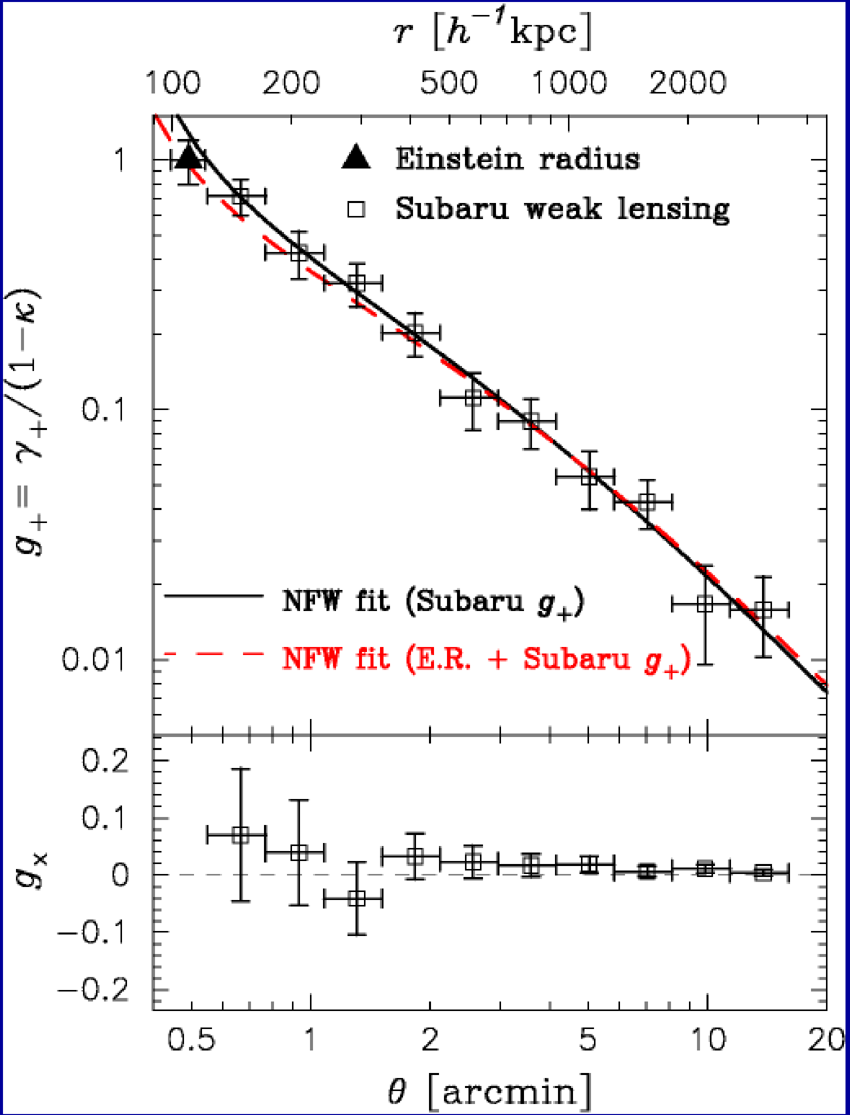

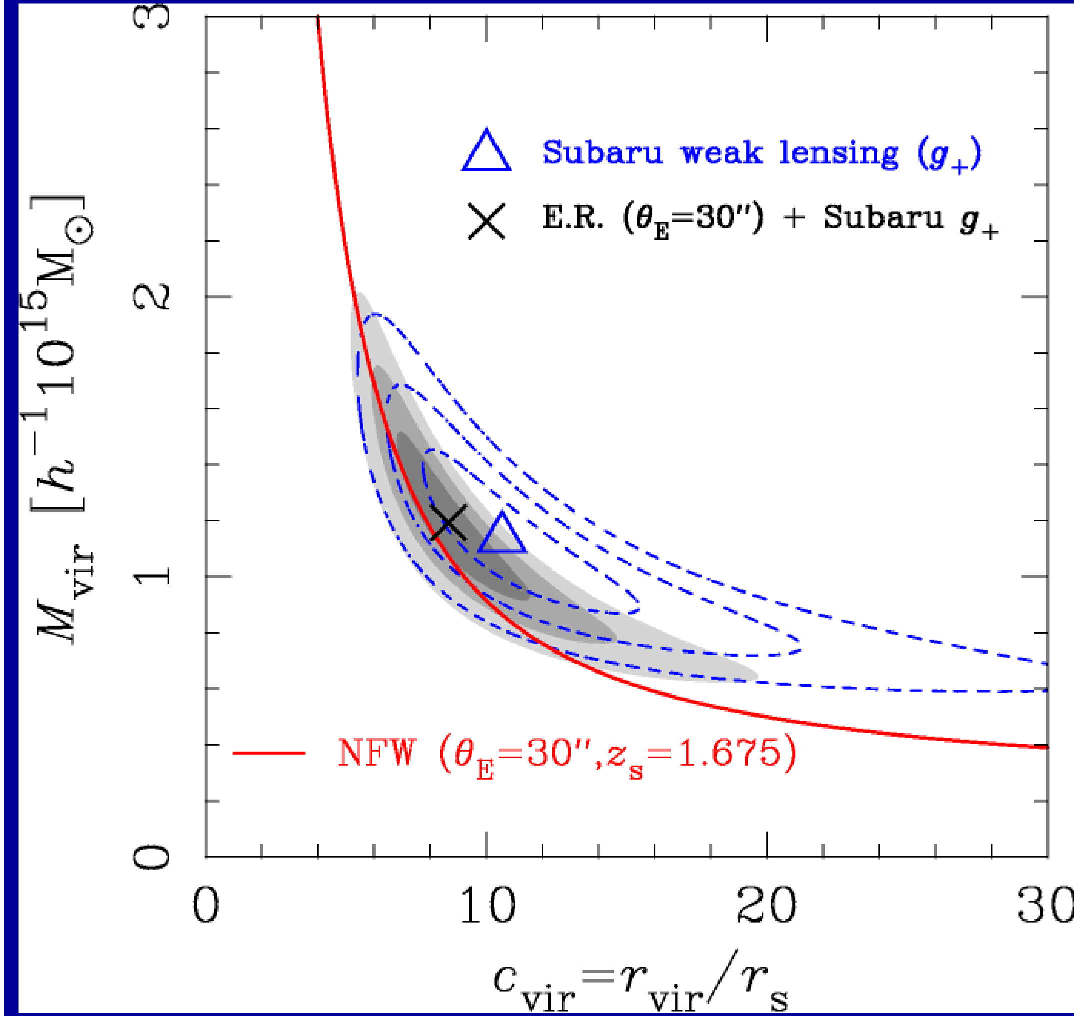

Umetsu, Medezinski, Broadhurst+ (2010)

Importance of AMiBA Frequency

SZE Frequency Spectrum and Coverage

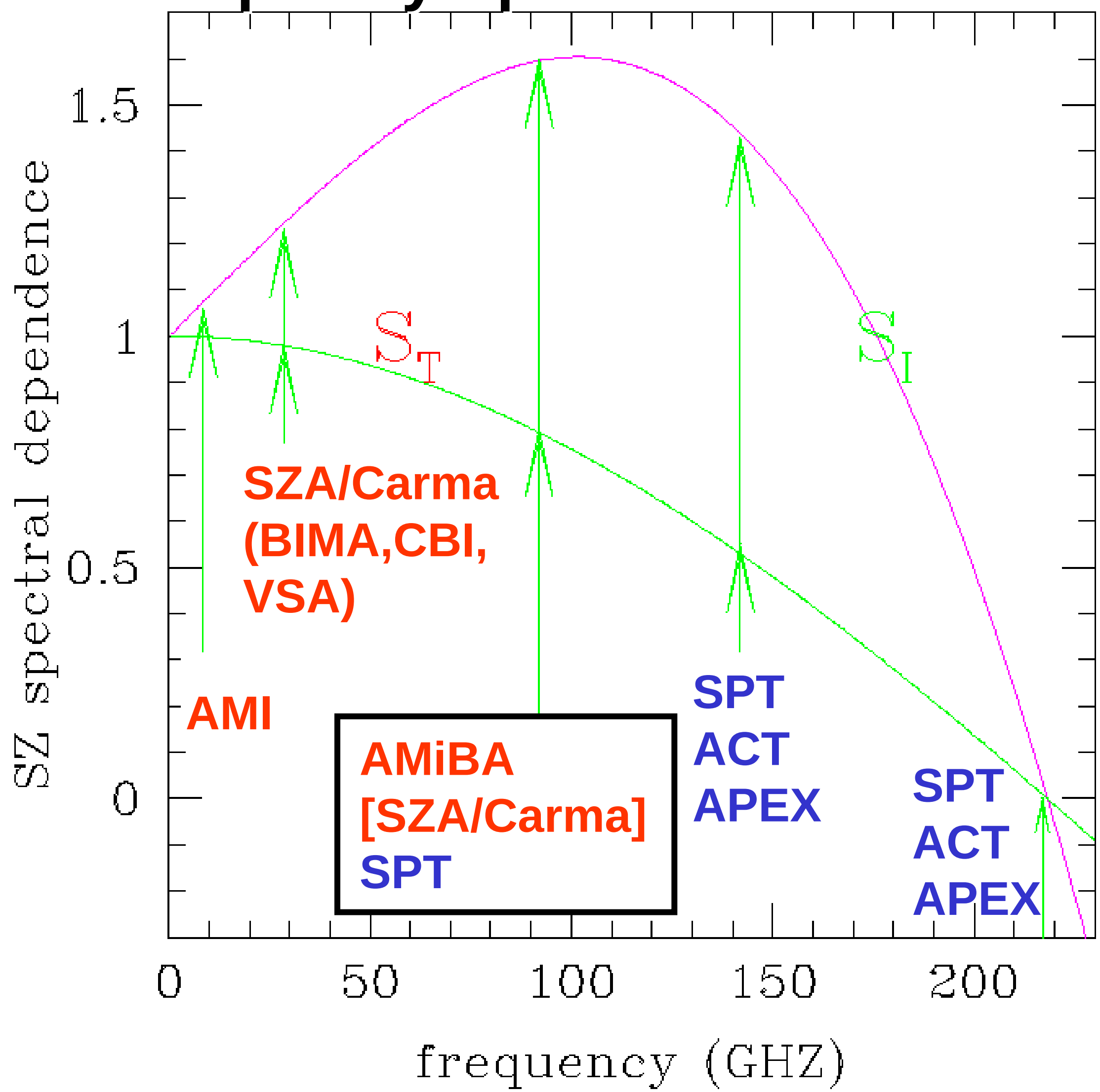

Red: Interferometer

Blue: Multi-pixel bolometer

– At 90-100GHz, relative SZE strength w.r.t. CMB and foreground emission is maximized: **optimal window**

– AMiBA is one of few leading SZE instruments operating at 3mm.

– AMiBA@3mm@Hawaii serves as a very unique SZE instrument for multi-wavelength SZE studies.

Fig from Zhang et al. 02

Why at 3mm?

Dust/Synchrotron foreground minimized

Typical SEDs of Galaxies

Other CMB interferometers:

CBI (@30GHz)

AMI (@15GHz)

SZA (@30/90GHz)

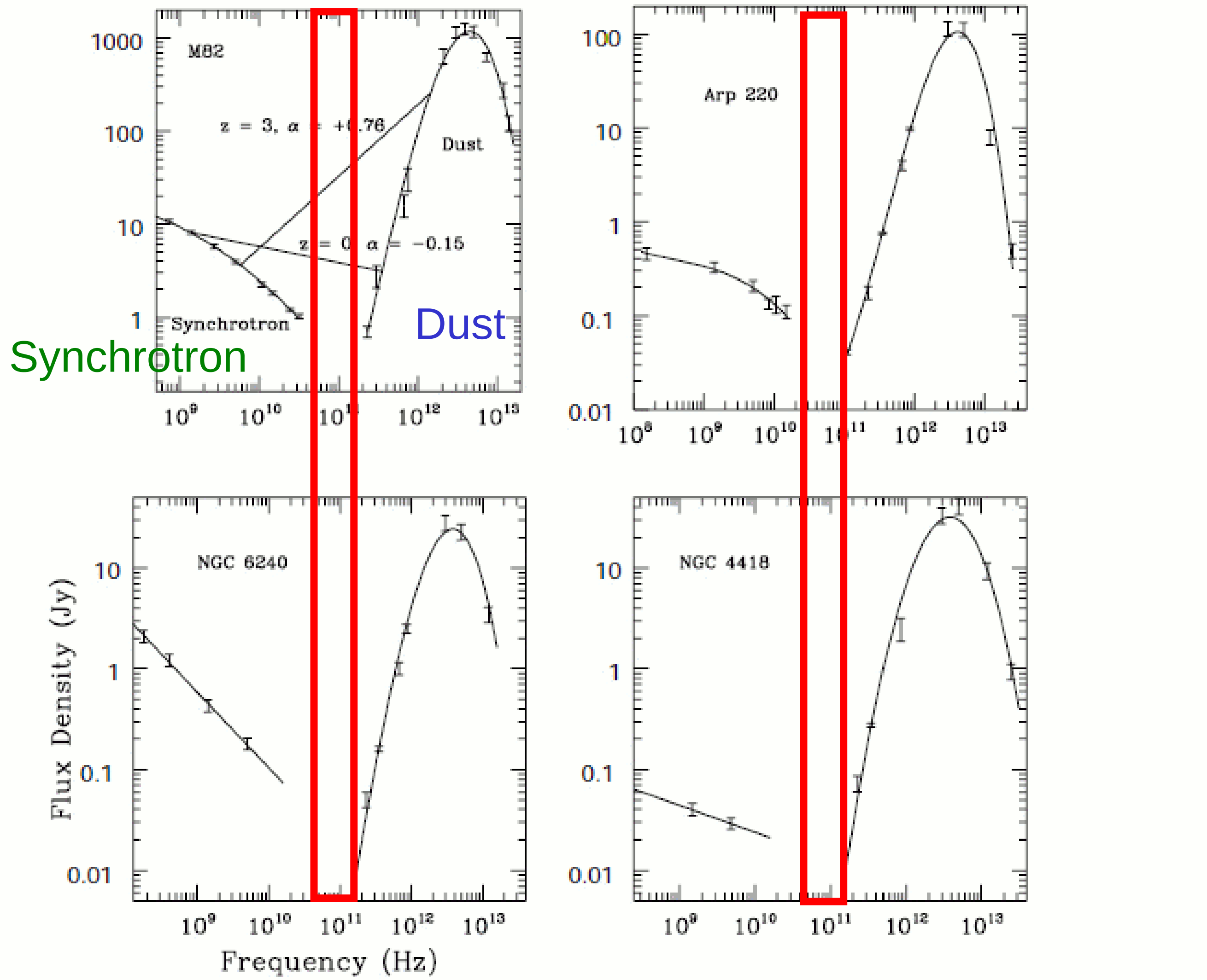

FIG. 1.—Data points show the radio through infrared spectral energy distributions of four representative galaxies from our sample of 17 listed in Table 1. The data are obtained from NED (*IRAS* data points), the NRAO VLA Sky Survey (Condon et al. 1998), the Westerbork Northern Sky Survey (Rengelink et al. 1997), and from Rigopoulou et al. (1996), Benford (1999), and Lisenfeld et al. (1999). The solid curves show polynimial fits to the data. For the M82 spectrum, the straight lines indicate the spectral index that would be derived for the source at $z = 0$ and $z = 3$ between observing frequencies of 1.4 and 350 GHz.